HYDROGEOPHYSICAL CHARACTERIZATION OF SWINE EFFLUENT AMENDED SOILS IN MANTLED KARST

By

JON JAY FIELDS JR.

Bachelor of Science in Geology

Oklahoma State University

Stillwater, Oklahoma

2014

Submitted to the Faculty of the
Graduate College of the
Oklahoma State University
In partial fulfillment of
The requirements for
The Degree of
MASTER OF SCIENCE
December, 2016

HYDROGEOPHYSICAL CHARACTERIZATION OF

SWINE EFFLUENT AMENDED SOILS

IN MANTLED KARST

Thesis Approved:

Dr. Todd Halihan

Thesis Adviser

Dr. Javier Vilcaez

Dr. Natascha Riedinger

ACKNOWLEDGEMENTS

I must start by thanking the Big Creek Research and Extension Team (BCRET), out of the University of Arkansas, who made all of this possible in the first place. It is not only the funding I thank them for, but also the experience this has provided me. Many of the various field assistants who helped along the way deserve a thank you as well, but especially Kelly Sokolosky and Timothy Glover for the continued effort put in to assist in my strenuous data collection. I would also like to thank the land owners in Mount Judea, Arkansas and the people of the state of Arkansas for being gracious hosts and willing participants.

I am grateful to my committee members for their assistance, time, and effort. I have to thank Dr. Halihan, whom without his guidance, none of my opportunities would be possible and that is something I cannot ever fully repay. I honestly could not have asked for a better teacher, life advisor, or friend. Most don't understand the dedication he has to each of his endeavors and how, regardless of the bumps in the road, his efforts shine through it all. This makes him one of Oklahoma State Universities most valued researchers and professors. I must mention his wife, Martha Halihan, for all she does for him (and subsequently me). The whole Halihan family has been exemplary and I am forever thankful for their hospitality. Dr. Javier Vilcaez and Dr. Natascha Riedinger provided a much needed sounding board for those areas where I lack expertise. Your time and patience with my work and questions has been invaluable and I appreciate it. Dr. Brian Carter helped get us off the ground, or topsoil rather. His willingness to help teach a very integrated science in such an effective manner so that we could continue with our work and interpretation did not go unnoticed. Since meeting Dr. Carter, I have suggested

several students take his courses due to his excitement about the topic and his expressed joy teaching it to a geologist. He is a model researcher and an asset to Oklahoma State University and I truly appreciate his time.

My most loving thank you goes out to my wife, Kayla Fields whom, without her patience, I would not have had the opportunity to complete this degree. She of all people, knows the trials I've been through and she's stuck by my side throughout it all. I must also thank my personal friends and family, looking at you Cullen Pickens, Tim Janousek, Sean Hussey, and Ethan Scott. There have been many days and nights where their support has either pushed me along, allowed me to enjoy the moment, or gotten me out of a rut. I appreciate all of you who have been in my life thus far. My parents, Jon Jay Fields Sr. and Kristi Michelle Fields, deserve high praises for teaching me my morals and work ethic. Not a day goes by that I don't rediscover a personal tool that was passed down many years ago. They are the reason that I am who I am, jokes and all. My brother Ryan Fields also deserves an acknowledgement, for without him, I would not know how to defend my point of view nor value my personal relationships in life.

Lastly, I need to acknowledge the two places that have allowed me to succeed at life. My hometown of Lawton, Oklahoma and Oklahoma State University. My hometown is a great place that has both toughened me up and taught me humility. Oklahoma State University has been a dream come true experience. Oklahoma State offers resources that make typical research boundaries vanish. Whenever I needed something I constantly found myself thinking "the university has to have this one, right?" Sure enough, I'd find my needs were met. The culture at Oklahoma State University magnifies the "Oklahoma Standard" and I am proud to call myself a Cowboy. Go Pokes!

Acknowledgements reflect the views of the author and are not endorsed by committee members or Oklahoma State University.

TABLE OF CONTENTS

Chapter Page

LIST OF TABLES

Table Page

LIST OF FIGURES

Figure Page

CHAPTER 1

1.0 INTRODUCTION

1.1 Importance

Accurately understanding the migration of swine lagoon effluent in the subsurface helps protect water sources from contamination benefiting both the public and private sectors. In riparian zones, knowing the transport of swine lagoon effluent applied to fields for disposal allows the understanding of potential environmental impacts. Characterizing transport of these materials in mantled karst is critical as the soil layer can be thin and rapid transport pathways can exist in the bedrock or epikarst zones.

1.2 The Problem

The problem being addressed is swine effluent amended soils within a mantled karst. Current knowledge gaps include understanding the spatial migration of swine lagoon effluent in the subsurface and the geophysical characterization of swine lagoon effluent applied to soils. To characterize swine effluent transport within a mantled karst system, this thesis will measure the electrical properties of the subsurface, characterize soil properties at the surface, and use reactive transport modeling to evaluate three sites near Mount Judea, Arkansas.

The three test sites are selected based on the amount and timing of effluent application to provide a range of sites to evaluate. These sites coincide with additional surface water quality monitoring on the fields by the University of Arkansas Big Creek Research and Extension Team

and access to the sites was granted by the landowners. The positions of the sites are representative of fields adjacent to Big Creek and which are permitted to receive swine effluent.

I hypothesize that swine lagoon effluent field applications in a mantled epikarst can be determined through electrical resistivity data observing an increase in electrical conductance of the applied soil. This will be tested with chemical and physical soil characterization and numerical modeling of the electrical and chemical properties of the soil zone.

1.3 The Objectives

Several of the objectives of this thesis were conducted as part of the work detailed in the report Electrical Resistivity Surveys of Applied Hog Manure Sites, Mount Judea, AR: Final Report (Fields and Halihan, 2016) and will utilize the data collected during that work. Completed objectives included:

- Pseudo 3D Electrical Resistivity Imaging (ERI) surveys were conducted to delineate the boundaries between the soil, epikarst, and competent bedrock to provide the electrical structure of the stratigraphy of the site,
- Depth to the local water table was determined using stream elevation and epikarst wells,
- Soil depth was determined by previously bored observation wells,
- Single 2D ERI surveys were conducted on each site to evaluate correlations between bulk electrical and physical soil properties for a set of application time periods,
- Soil solids sampling and analysis was conducted on each site for grain size, mineral analysis, and chemical properties,
- Soil water sampling was conducted on each site for chemical properties, and
- Numerical modeling was conducted to create a site model to predict swine lagoon effluent movement on amended soils.

The ER data were integrated with soil sampling analysis results, differential GPS, and statistical analysis to generate site characterization.

1.4 Electrical Resistivity Imaging

Electrical resistivity imaging (ERI) provided a good method to understand the distribution of fluids and rock properties in the subsurface environment, especially in the presence of fractures (Bolyard, 2007; Gary et al., 2009; Halihan et al., 2009). The method allows an electrical image to be created of the subsurface, which typically provides a meter-scale electrical resistivity dataset utilized to evaluate heterogeneity and fluid distribution. Improvements in sensitivity generated by the Halihan/Fenstemaker method (OSU Office of Intellectual Property, 2004), allow greater differentiation of these signatures (Miller et al., 2014). In a field setting, this results in a two-dimensional mapping of subsurface electrical properties in vertical cross sections. Data interpolation was utilized to construct horizon maps at various depths below the surface.

Figure 1 - Electrical resistivity equipment during data collection (12.17.14)

1.5 Soil Sampling

Soil sampling transects in each field provided confirmation data to support the geophysical datasets. Soil sampling has been used for obtaining the chemistry and characteristics of soils (Anderson, 1960; Corwin and Lesch, 2005; Schoenau, 2006). These data were compared against the electrical resistivity data to evaluate how the soil physical and chemical properties affected the geophysical signatures observed for the sites.

1.6 Numerical Modeling

Numerical modeling is a good method for visualizing possible scenarios of the system without physically changing the system. The process involves building and applying known datasets to the appropriate reaction and transport equations, generating predictions about the system's behavior and verifying the predictions through comparisons against experimental data.

1.7 Project Statement

This research utilized a hydrogeophysical investigation of three sites along Big Creek near Mount Judea, Arkansas using electrical resistivity and soil sampling datasets to evaluate if applied effluent provided an electrical signal that could be utilized to monitor transport. It will describe the field sites and the literature available for the methods utilized and the properties of applied swine effluent. The results of the study will be presented with the geologic and hydrogeologic structure evaluated from the electrical data. The soil data results will be presented and correlations between the datasets will be evaluated and discussed. Conclusions about the electrical resistivity properties of the sites and their implications for effluent transport in a mantled karst will be presented.

CHAPTER 2

2.0 LITERATURE REVIEW

Soil science and hydrogeophysical literature uses similar concepts, but with varying terminology. Some terms have somewhat different meanings, so a few key terms must be mentioned to clarify how they are used in this work. Electrical resistivity data (ER) refers to data generated by measuring the current potential between two electrodes, or apparent resistivity, of the subsurface (both soil and bedrock) and inverting the measurements to obtain model ER data; Electrical Resistivity Imaging (ERI) is the method that obtains the resistivity data. Soil electrical conductivity (EC_a) is a measurement of soil solids, liquids, and a combination of the two (Dane and Topp (eds), 2002); and fluid electrical conductivity (fluid EC) is a measurement of the electrical conductivity of free water in a stream or well of a 1:1 soil to water extraction (Corwin and Lesch, 2005; Dane and Topp (eds), 2002; Samouëlian et al., 2005; Van Nostrand and Cook, 1966). This literature review documents electrical geophysics applied to karst and soil sciences, soil amendments with fertilizers and swine lagoon effluent, and reactive transport modeling. Geophysics has been used for collecting bulk measurements of subsurface properties.

2.1 Geophysics on karst and soils

Detection of caves and sinkholes is a major point of investigation for near-surface geophysical studies in karst areas. Epikarst and karst have been evaluated using Ground Penetrating Radar (GPR) (Benson, 1995; Chamberlain et al., 2000), ERI (Gary et al., 2009; Halihan et al., 2009; Martinez-Lopez et al., 2013; Mihevc and Stepisnik, 2008, 2012; Schwartz

and Schreiber, 2009; van Schoor, 2002; Zhou et al., 2000; Zhu et al., 2011), and some combination of other geophysical techniques paired with ERI (Carriere et al., 2013; Kaufmann et al., 2011; Leucci, 2006; Pellicer and Gibson, 2011). The size and depth of the karst features are key for detection of those features across any array or setup (Martínez-López et al., 2013). Bolyard (2007) detailed a fracture network below a landfill in Northwest Arkansas using ERI. Karst systems can be shallow or deep depending on the maturity of the weathering profile and thickness of the bedrock. Saturated caves are typically conductive anomalies, of which the extent depends on the fill in the cavity (Gary et al., 2009). When filled with air, these caves are highly resistive anomalies (van Schoor, 2002; Zhu et al., 2011). When knowing the depth to bedrock is required, GPR is most useful and consistent for delineating sedimentary beds from competent bedrock in lowly saturated or unsaturated medium (Tsoflias et al, 2001). ERI is more useful in discriminating between competent bedrock and the overlying, more porous soil material as it can differentiate between higher and lower porosities in a saturated medium. Pellicer and Gibson (2011) selected the depth to bedrock where they found the highest electrical gradient and supported it with GPR surveys.

Shallow, high resolution studies have been conducted for soil evaluation since the 1970's at depths above bedrock. ER and EC_a rely heavily on the soil properties (Brunet et al., 2010; Corwin and Lesch, 2005; Neilsen et al., 1973; Robain et al., 2006; Samouëlian et al., 2005). The most crucial set of parameters to the electrical conductivity of shallow surveys are clay content, moisture profile, moisture salinity, and moisture temperature (McNeill, 1980). Clay content and electrical conductivity exhibit a positive relationship (electrical conductivity rises with clay content) which is extremely important for soils studies focused on grain size analysis (Gaio et al., 2002; Johnson et al., 2001; Oh et al., 2014; Sudha et al., 2009). Other physico-chemical and biological properties that affect EC_a are mineralogy, bulk density, and microbial biomass (Atekwana and Atekwana, 2010; Johnson et al., 2001).

Electrical resistivity imaging does have challenges associated with the technology. Several different parameters affect electrical conductivity of the subsurface and knowing which to evaluate is extremely important as the difficulty to determine exact causes increases with larger scales. Size of subsurface features, such as karst voids, are also extremely important. Some authors note that when the size is too small or other, stronger, electrical signatures are present, then finding karst features or delineating from other features become increasingly difficult (Allred et al., 2003; Corwin and Lesch, 2005; Oh et al., 2014; Samouëlian et al., 2005; Sudha et al., 2009; Zhu et al., 2011). Although several studies have been conducted evaluating bulk electrical resistivity using geophysical tools and apparent soil electrical conductivity with hand held probes, few have used ERI and soil sampling to evaluate amended soils (Allred et al., 2003).

2.2 Amended Soils

Since the mid-1800s, research has been conducted to understand plants nutritional requirements and soil fertility (Anderson, 1960). Important parameters for soils include nutrient availability, organic matter (mainly carbon and nitrogen), and soil pH (Brady and Weil, 2002). A quality soil depends on the soil type and geographic location of the soil. Animal manures are useful for increasing many properties that make up a quality soil (Davis and Zhang, 2001; Espinoza et al., 2016; Mitchell, 1995; Sharpley et al., 2016; Zhang, 1998, 2002, 2016; Zhang and Schoenau, 2006; Stiegler, 1998). However, fields are typically over fertilized due to a lack of prior soil testing to determine the current field conditions and result in constituents leaching from the soil profile (Gollehon et al., 2001; Schoenau, 2006; Zhang and Stiegler, 1998). More stable and consistent texture-dominated systems can become salinity-dominated systems given high enough concentrations of salts within soil applications. Each field has different initial concentrations of constituents while plants on those fields require different nutrients to thrive, generally there is no “one size fits all” approach to soil amendments and that concentrations and

requirements of fertilizers, manures, fields, and plants should all be determined before any amendments are made (Schoenau, 2006; Zhang and Stiegler, 1998).

2.2.1 Swine Lagoon Effluent

Animal effluent is a byproduct of animal farms and a concern for CAFOs (concentrated animal feeding operations) due to the significant resources required for environmental management of the waste. The effluent is also a valuable source of organics and nutrients for plants, cropland, and pastures (Broetto et al., 2014; Gollehon et al., 2001; King et al., 2015). Different animals have different agronomic and environmental impacts from differences in nutritional needs of the animal, dietary factors, and other growing conditions (DeRouchey et al., 2009). Waste storage is important for managing not just the physical aspect of waste, but the chemistry of the waste for impacts to the storage unit and wherever it may end up (Choudhary et al., 1996; DeRouchey et al., 2009; Schoenau, 2006) especially as the large CAFOs get even larger (Gollehon et al., 2011). A significant problem for CAFO farmers is the amount of waste generated by the facility and ways to reduce waste treatment costs. This is often accomplished by applying effluent to fields of farmers who own nearby fields. Several studies have shown increases in both macro- and micro-nutrients after effluent applications (Broetto et al., 2014; DeRouchey et al., 2009; Gollehon et al., 2001; Hountin et al., 1997; Marr and Facey, 1995; Schoenau, 2006) but this isn't always beneficial for the crops or pasture, as the application rates can be too low to provide optimal nutrients for plant growth (Broetto et al., 2014; Gollehon et al., 2001) and responses in soil samples may not show after an initial application but only after a continued series of applications (Hountin et al., 1997; King et al., 2015). Low concentrations of nitrogen in the effluent may be caused by volatilization prior to field application. The extent of nitrogen's change in concentration depends on the type of storage and application (Adeli et al., 2002, 2008; Choudhary et al., 1996; Gilley, 1995; Mallin and Cahoon, 2003).

2.2.2 Isotopic and Chemical Signatures

Well-studied chemical indicators of an applied effluent site vs a non-applied site include a wide range of parameters (Table 1). These indicators can be broken into two groups, ions found in soil solids and fluids and the more complex constituents such as organics and microbial activity.

Table 1 - Literature compilation of indicators for an applied effluent site vs a non-applied site.

Constituent measured	Author, date
Organic Content	Anderson, 2012; Broetto et al., 2014; King et al., 2015; Marr and Facey, 1995; Mitchell and Everest, 1995; Schoenau, 2006; Wallenius et al., 2011
Microbial Activity	Deng et al., 2006; Iyyemperumal and Shi, 2008; Schoenau, 2006; Wallenius et al., 2011
Isotope Signatures	Fogg et al., 1998; Kendall and McDonnell, 1998; Krietler, 1975, 1979; Wolterink et al., 1979
Nitrogen, Phosphorus, and Potassium (NPK)	Broetto et al., 2014; Carpenter et al., 1998; Hannan, 2011; Iqbal and Krothe, 1995; Marr and Facey, 1995; Mallin and Cahoon, 2003; Racz and Fitzgerald, 2000; Reddy et al., 1980; Schoenau, 2006; Smith et al., 2007; Vadas et al., 2007; Wallenius et al., 2011
Calcium and Magnesium	Akay and Doulati, 2012; Hannan, 2011; Plaza et. al, 2004
Metal Content	Akay and Doulati, 2012; Broetto et al., 2014; Comegna et al., 2011; Lukman et al., 1994; Murdock and Lowe, 2001; Perelomov et al., 2011; Pérez-novo et al., 2011; Racz and Fitzgerald, 2000; Schoenau, 2006
pH	Choudhary et. al, 1996; Comegna et al., 2011; DeRouchey et. al, 1999; Frankenberger and Dick, 1983; Hannan, 2011; Klimek, 2012; Lukman et al., 1994; Marr and Facey, 1995; Plaza et. al, 2004; Racz and Fitzgerald, 2000; Schoenau, 2006; Smith et. al, 2007; Suhadolc et. al, 2004; Turner et. al, 2010

Swine effluent impacts on soil can be determined using soil sample analysis of basic fluid parameters, such as EC or pH, or measurements of ions in the soil. Racz and Fitzgerald (2000) report that EC of the manures did not correlate with salts such as sodium or chloride, but rather with the variation in inorganic nitrogen. Adeli et al. (2002) found nutrient concentrations increased with increased swine lagoon effluent application. However, after long-term application (Adeli et al., 2008), soil EC and total carbon increased across all fields while nitrogen, phosphorus, and zinc were higher only on less-alkaline soils. An unexpected finding in Adeli et al. (2008) was that soil pH decreased after long-term applications because Schoenau (2006) points out pH typically increases after long-term effluent applications. These results indicate the dependency of pH's upon organic matter content and other buffering agents in the effluent. Calcium, magnesium, potassium, and pH have been shown to have elevated levels in the soil from anthropogenic sources (Racz and Fitzgerald, 2000; Schoenau, 2006). Zinc and other metals have been supplied as additives to swine feed and can be detected in their effluent as having increased metals concentrations when compared to those without the additive (Akay and Doulati, 2012; Broetto et al., 2014; Comegna et al., 2011; Klimek, 2012; Lukman et al., 1994; Murdock and Lowe, 2001; Perelomov et al., 2011; Pérez-novo et al., 2011; Racz and Fitzgerald, 2000; Schoenau, 2006; Suhadolc et. al, 2004).

A significant amount of soil literature focuses on organic matter and fertilizer components in soil. Organic matter is beneficial for plants and microbial communities and increases with manure applications, lower temperatures, higher precipitation, and poor drainage. For fertile soils the OM should be upwards of 5% and reside in the topsoil (Mitchell and Everest, 1995). Organic carbon and total nitrogen correlate well with microbial activity (Deng et al., 2006; Frankenberger and Dick, 1983; Plaza et al., 2004; Schoenau, 2006; Wallenius et al., 2011) as does soil pH (Iyyemperumal and Shi, 2008). The nitrogen isotope ratio ($\delta^{15}N$) is important for evaluating signatures of human and animal effluent and has been found to be between 15‰ –

20‰ for animal effluent signatures in soils (Fogg et al., 1998; Krietler, 1975, 1979; Wolterink et al., 1979). Other nitrogen isotope signatures, such as for natural soils and rainfall, can vary, but are generally well below 15‰ (Aly et al., 1981; Aravena et al., 1993; Black and Waring, 1977; Bremner and Tabatabai, 1973; Freyer, 1978, 1991; Garten, 1992, 1996; Gormly and Spalding, 1979; Heaton, 1986, 1987; Heaton et al., 1997; Hoering, 1957; Kohl et. al, 1971; Moore, 1977; Paerl and Fogel, 1994; Shearer et al., 1974, 1978). Well-drained sites and denitrification both impact the nitrogen isotopic signatures as well as nitrogen evolution after application to the soil (Kendall and McDonnell, 1998). Phosphorus and nitrogen are both highly studied nutrients because of their negative environmental impacts when in high concentrations and during runoff events (Carpenter et al., 1998; Deng et al., 2000; Hountin et al., 1997; Iqbal and Krothe, 1995; Kleinman et al., 2006; Reddy et al., 1980; Schimel and Bennett, 2004; Sharpley, 1985, 1995; Smith et al., 2007; Vadas et al., 2007; Vitousek et al., 1997; Yadav, 1997). Both elements chemical signatures are commonly studied in swine lagoon effluent research.

2.2.3 Reactive Transport

Numerical modeling has given scientists a way to test hypotheses at a fraction of the cost of field work, with the ability to conduct numerical experiments quickly, and to alter the experiment to fit many different possible scenarios. Subsurface fluid flow has been at the center of numerical modeling in the geosciences for decades (Berkowitz, 2002; Chen and MacQuarrie, 2004; Celia et al., 1989; Steefel et al., 2005; Xu et al., 2003, 2010). And through the years biogeochemical modeling has evolved to offering numerical simulations of reactive chemistry during multiphase flow of fluid and/or heat, within porous and fractured media (Xu et al., 2010). TOUGHREACT specifically, can simulate in “three-dimensions, changes in pressure, temperature, water saturation, ionic strength, and pH and Eh” and has been demonstrated as conducting simulations on the biogeochemical cycling of metals (Xu et al., 2003, 2010). Steefel et al. (2005) simplify the history of reactive transport modeling into two historic “threads”: on

one side is the physical model that attempts to perfect the mass and heat aspects of the model, but treat the biogeochemical aspect with simple equations; the other side is the opposite, the geochemical model uses some sort of equilibrium component to attempt to perfect the biological and chemical aspects of the model, but separate the physical characteristics entirely. They also state that the current state of the science allows for a single program to include "hydrology, geochemistry, biogeochemistry, soil physics, and fluid dynamics". Here we can marry several studies together to grasp a better understanding of subsurface reactions.

The controlling parameters in a soil column include solute concentrations, competing species, distribution coefficients, moisture and air content, and porous media bulk density (Chen and MacQuarrie, 2004). The pH of the soil is extremely important for reactive transport of metals, as mobility increases with acidity (Luxton et al., 2013). Specifically for the sorption of zinc, it is highly dependent upon pH, clay content, Cation Exchange Capacity (CEC), and carbonate presence (Akay and Doulati, 2012; Comegna et al., 2011; Lukman et al., 1994; Luxton et al., 2013; Murdock and Lowe, 2001; Xu et al., 2010). Clay content has been found to be very important with certain clay structures, 2:1 and 2:2:1, allowing for higher levels of sorption (Luxton et al., 2013). CEC has been found to be higher when there is more soil OM, which leads to higher adsorption (Lukman et al., 1994).

One focus of soil studies and modeling is rainfall intensity and its effect on nutrient transport. Smith et al. (2007) found that simulating rainfall within 1 week of a fertilizer application highly increases the chance for runoff. When rainfall occurs on soils with higher initial moisture content, such as during the spring months, higher desorption and surface runoff has been recorded (Kleinman et al., 2006). Likewise, when initial soil moisture content is low, it is more influential on runoff than is rainfall intensity, although typically with increased rainfall intensity comes higher runoff (Kleinman et al., 2006). Sharpley (1985) determined the depth to which runoff interacts with the surface soil increases with rainfall intensity and soil slope. Under

heavy rainfall events on a slope, there is a better chance of reactive transport occurring within the first few centimeters. Although denitrification modeling require more input (Heinen, 2006; Maggi et al., 2008), nitrogen in general relies heavily on baseline precipitation and soil texture (Gu and Riley, 2010) but can be completely washed through a system given sufficient amount of rainfall (Iqbal and Krothe, 1995). Phosphorus is expected to be present in higher levels near the surface as it has been shown as a significant factor during runoff events due to its sorption-desorption near the surface (Vadas et al., 2007). During more intense storms, not only is runoff present, but constituents can be also flushed thoroughly through the system (Iqbal and Krothe, 1995; Sharpley, 1985; Smith et al., 2007).

CHAPTER 3

3.0 SITE DESCRIPTION AND SELECTION

Three test sites (Fields 1, 5a, and 12) near Mount Judea, Arkansas, United States were used to evaluate applied effluent signatures over time (Figure 2). These three sites were selected to coincide with additional monitoring on these fields by the University of Arkansas Big Creek Research and Extension Team. Access to the sites was granted by the landowners. The positions of the selected sites are representative of fields adjacent to Big Creek, which are permitted to receive swine lagoon effluent: the fields were selected as a background site (Field 5a) that currently receives mineral fertilizers and poultry litter, a site which has received one application of swine lagoon effluent approximately one year prior to sampling (Field 12), and a site, which has received two applications of swine lagoon effluent with the most recent being approximately a month prior to sampling (Field 1). This section will describe the geologic and hydrologic settings of the three test sites.

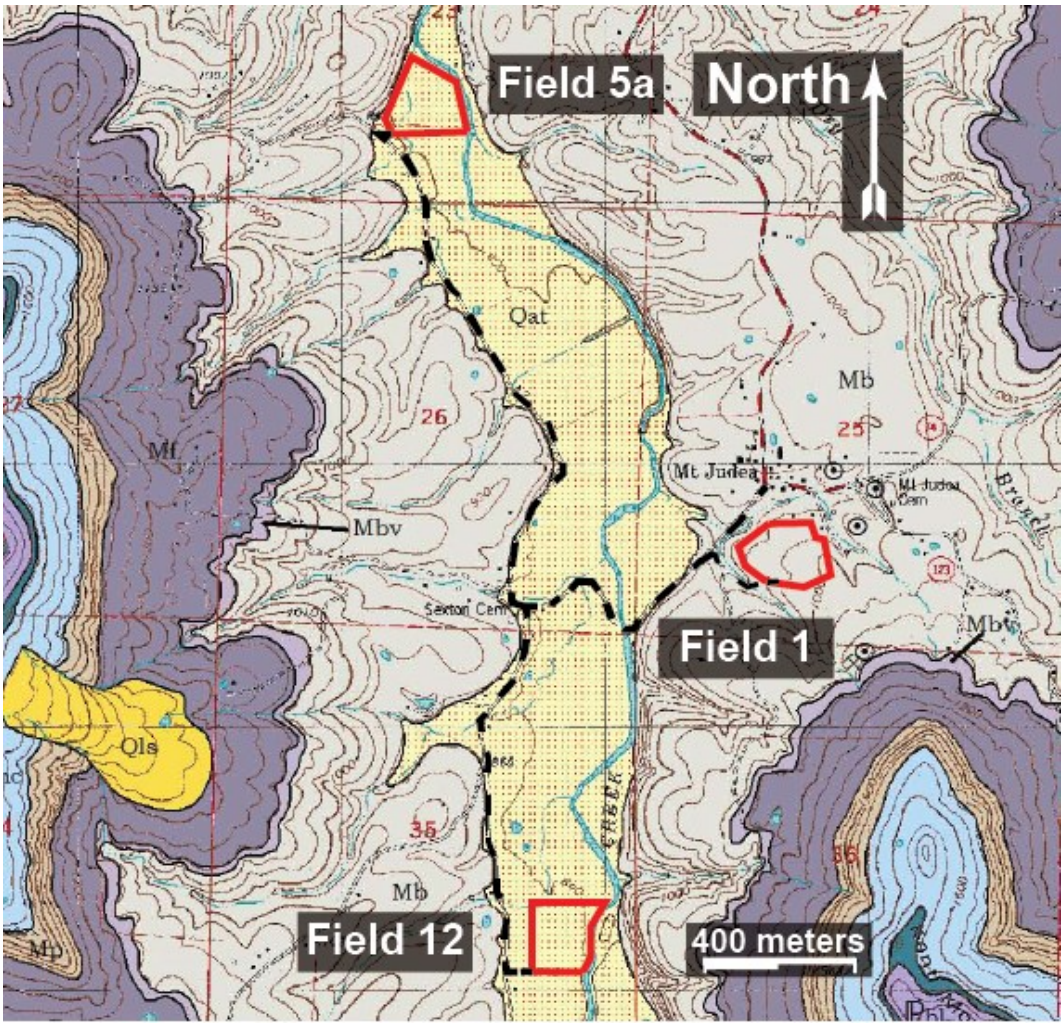

Figure 2 – Site map indicating the three fields (Field 1, 5a, and 12) in red and roads leading to these sites in dashed black lines. The background map is the geologic map of the Mt. Judea Quadrangle, Newton County, Arkansas (Chandler and Ausbrooks, revised 2015).

3.1 Geologic Setting

The geologic setting for each site is a mantled epikarst (soil over epikarst over competent carbonate bedrock) (Klimchouk et al., 2004; Williams, 2008). Fields 5a and 12 include thin Quaternary alluvium soil deposits on the epikarst, while Field 1 is located on a thin, locally derived soil.

The Boone Formation is the underlying bedrock for each of these sites. It is an Early Mississippian limestone found in the Ozark regions of Eastern Oklahoma, Southern Missouri, and Northern Arkansas where karst dissolution features are common (Ferguson, 1920). This formation averages 90 – 120 m (300 – 400 feet) thick (Ferguson, 1920). The Boone Formation is a gray, fine to coarse-grained fossiliferous limestone with interbedded dark and light chert. The basal unit of the Boone Fmt. in the area is the St. Joe Limestone (Ferguson, 1920). The St. Joe Fmt. is a fine-grained, crinoidal limestone containing some smoothly bedded chert and displaying coarse bioclastic texture. The color is generally gray but can be red, pink, purple, brown, or amber. Thin calcareous shales can be found in sequences throughout the St. Joe. The base of the St. Joe contains phosphate nodules within a green shale or conglomerate and is disconformable in most places. At a few locations, basal sandstone is found at the base of the St. Joe Limestone. The basal sandstone is a fine to medium-grained, moderately sorted, sub-rounded to rounded sandstone. It is white to light gray and tan on fresh surfaces, thin to thick bedded, and contains phosphate nodules and white to light gray chert. It is generally up to 3.5 m (12 feet) thick (Ferguson, 1920).

An epikarst zone, fractured and weathered bedrock, lies above the unweathered Boone limestone bedrock and extends upward to the base of the soil zone (Klimchouk et al., 2004; Williams, 2008). This zone is generally a domain with faster fluid flow and greater water storage than the unweathered bedrock, with distinct saturation at the soil and epikarst boundary and again at the epikarst and karst boundary (Perrin et. at., 2003). General epikarst porosity ranges from 1% (Smart and Friederich, 1986) to 10% (Williams, 1985) and averages about 10 – 15 m (33 – 49 feet) in depth (Klimchouk et al., 2004).

Fields 5a and 12 (Figure 3 and Figure 4, respectively) share similar geologic settings adjacent to Big Creek (Figure 2). The soil series for these fields is the Spadra Series and consists of clay, silt, sand, and gravel deposited by a stream system in the valley (Fowlkes et al., 1988).

Field 1 (Figure 5) is located on a hillside not far from Big Creek and the soil is derived primarily from the Boone Formation.

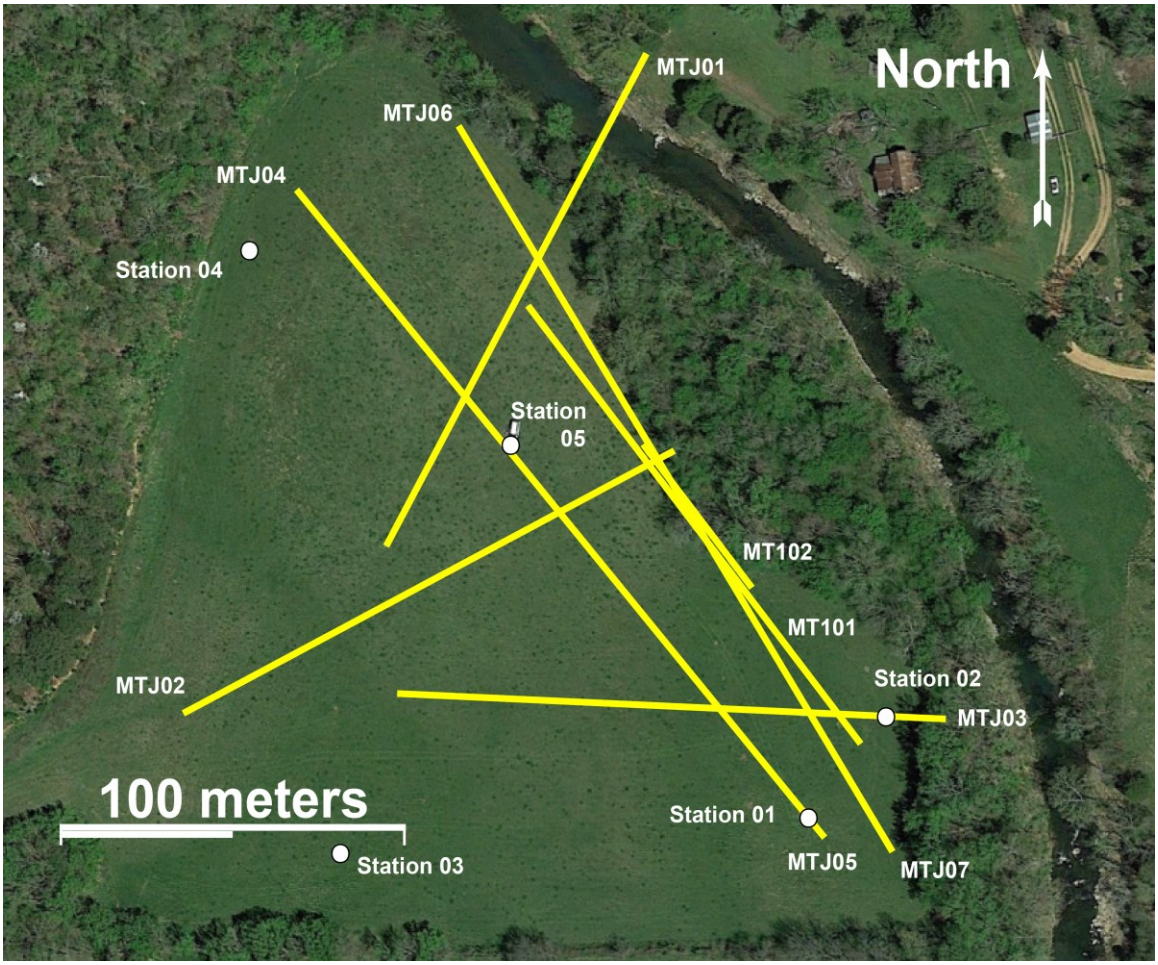

Figure 3 – Field 5a (background site) ERI transects collected during December 2014 and March 2015 are in yellow, shallow well locations (stations) also noted. Aerial photo obtained from Google Earth.

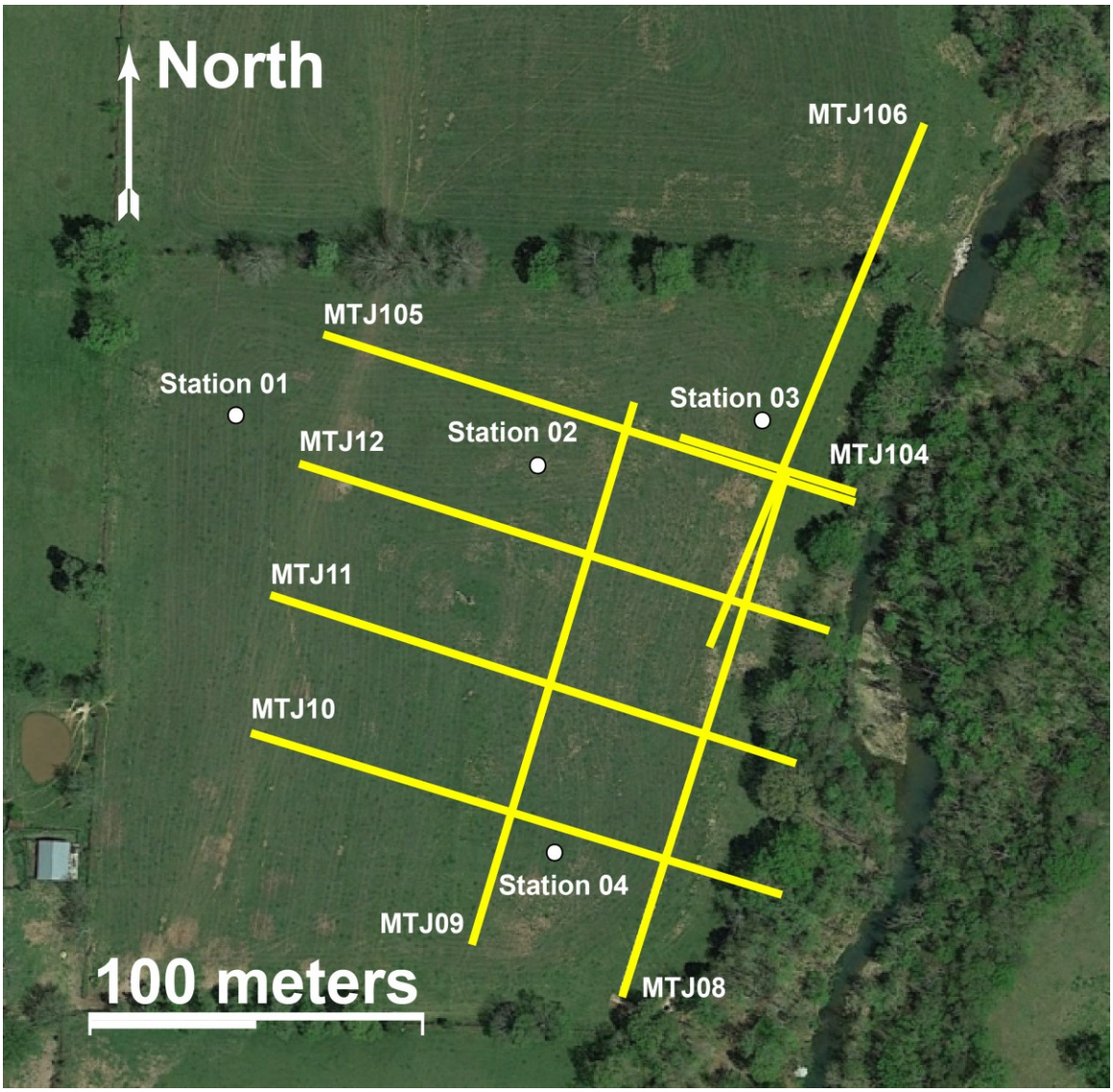

Figure 4 – Field 12 (application site) ERI transects collected during December 2014 and March 2015 are in yellow, shallow well locations (stations) also noted. Aerial photo obtained from Google Earth.

Figure 5 – Field 1 (recent application site) ERI transects collected during March 2015 are in yellow. Aerial photo obtained from Google Earth.

3.2 Hydrologic Setting

Flow through mantled epikarst generally consists of porous media flow through soil and potential for rapid flowpaths through the epikarst and bedrock zones. Understanding the storage and transmission properties of these three zones is essential to understanding the migration of nutrients from applied effluent in these areas. This section will discuss the hydrologic settings of the soil, epikarst, and bedrock zones, as well as the local water table and the application of effluent relative to the time of data collection.

The soil zones in an alluvial setting are often reworked stream deposits that have been mobilized several times since they were originally deposited. They are often highly variable in grain size and organic content. Silt-sized grains in Fields 5a and 12 should result in the ability of the soil to hold fluids for some period of time (Fowlkes et al., 1988; Perrin et al., 2003; Smart and Friederich, 1986). The soil zones in an epikarst environment are thin and often contain rock within the zone near the surface (Klimchouk et al., 2004; Williams, 1983, 2008). The soil zone consistency is sporadic as the hydrological processes erode areas at differing rates (Klimchouk et al., 2004). The soil and epikarst interface in Field 1 is very shallow, resulting in less soil filtering that the other sites prior to fluids entering into the epikarst zone (Klimchouk et al., 2004; Perrin et al., 2003; Smart and Friederich, 1986; Williams, 1983, 2008; Vanderhoff, 2011).

In geologic settings like northern Arkansas, the epikarst zone is a significant source of water storage and transmission and many springs have been tapped to support local communities (Galloway, 2004). These types of groundwater systems can include perched water tables, which exist above regional water tables. These are called perched because they are places where low permeability soil or bedrock layers hold water above an unsaturated zone. These generally produce springs on the side of a bluff or sometimes in an open field if the relief is high enough to expose this feature. The boundary of the soil zone with the epikarst zone is visible in some locations in the fields used for this study (Perrin et al., 2003). Perched features are not apparent at any of the sites. This zone is expected to have wide variability in flow rates and a high amount of storage (Williams, 2008). There can be slow seepage through weathered pores and pieces of less weathered bedrock, to relatively rapid flow through fractures and karst features. The electrical features measured at mantled karst sites generally indicate high porosity zones and the extent of weathering in these locations (Halihan et al., 2009; Pellicer and Gibson, 2011; Williams, 2008).

Flow through the bedrock will depend on the location of fractures or karst features. These flowpaths will most commonly be electrically conductive relative to the unweathered bedrock

beneath the water table. In settings with little dissolution and strong faulting or fracturing, the flowpaths will appear as linear features in ERI datasets (Halihan et al., 2009), but in the event of karst features, they can appear wider (Bolyard, 2007; Gary et al., 2009). Fractures or karst flowpaths present in the bedrock can be localized or, more often, follow larger regional trends.

The regional water table was not evaluated for this report but at the two sites on the alluvium, the local water table was shallow (a couple meters) during the investigation. For Field 5a, the depth to the local water table was approximately 1.5 m (5 feet) below the land surface. For Field 12, the local water table was approximately 2 m (6.5 feet) below the surface. The local water table was not detected in Field 1. Precipitation previous to and during the investigation resulted in both sites having moist to saturated soil conditions. The soil of Field 1 was saturated.

Swine lagoon effluent application periods and quantities were reported and used to determine the volume and time periods for applications. Field 5a did not have any known swine lagoon effluent application. Reports indicated swine lagoon effluent was applied to both fields 12 and 1. Field 12 received one treatment in April 2014 of 48,000 gallons (182 m^3) spread over 9.9 acres (40,064 m^2) for an application flux of 0.18 inches (0.5 cm) of applied manure. This application was eleven months prior to sampling for both ER and soil composition. Field 1 received four applications of applied manure. Total application was 82,000 gallons (310 m^3) over an average of 6.9 acres (27,923 m^2), which provides a total flux of 0.44 inches (1.1 cm) prior to sampling. The latest application before ERI and soil sampling was in January or February 2015 when 21,000 gallons (79 m^3) were applied to 7.3 acres (29,542 m^2) resulting in an event flux of 0.11 inches (0.3 cm) approximately a month prior to sampling. The applied material was electrically conductive fluid with reported conductivities ranging from 8,410 to 12,890 µS/cm.

CHAPTER 4

4.0 METHODS

As part of cooperative research, Oklahoma State University (OSU) designed and conducted electrical geophysical experiments to determine if geophysical signatures of applied effluent could be detected and utilized to evaluate transport of the effluent. Field methods included ERI surveys, topographic site surveying using differential GPS (global positioning system) techniques, and soil sampling along ERI surveys.

4.1 General Field and Laboratory Methods

These were the general methods used to collect the ERI, GPS, and soil sampling data. Site specific methods will follow the general descriptions of the methods used for the project.

4.1.1 Global Positioning System Surveys

Topographic surveys were required for generating the two-dimensional cross-sections produced from the ERI data as well as created a site topographic map. The Global Positioning System (GPS) used for site surveying was a Topcon Positioning Systems, Inc. HyperLite GNSS Base and Rover with Bluetooth connected handheld unit. Personal GPS units come to within approximately 3 m (10 feet) of a person's true location, but this commercial grade instrument provides locations to within approximately one centimeter (1/2 inch) of its true location. This instrument was set up by positioning a base receiver and utilizing a second mobile receiver to obtain data. Tree cover can be problematic for the Rover to obtain satellite data. At times, points

cannot be collected because the Rover was under too much tree canopy. This was the case on both sites near the stream (i.e., Big Creek) and along the site boundaries if tree canopy was dense. The majority of the data were collected in open field conditions, allowing good coverage of the ERI locations.

4.1.2 Electrical Resistivity Imaging Data

ERI data collection requires special instruments as well as transect planning. The ERI data collection instrumentation used was an Advanced Geosciences, Inc. (AGI) SuperSting R8/IP resistivity instrument. The instrument is a multi-channel earth resistivity meter with memory storage. The multi-channel design allows for measuring times to be decreased. The project design for Phase I from OSU was to use 56 electrodes at 3-m spacing (9.8 feet). This spacing allowed for detailed data collection at 1.5-m (4.9 feet) resolution for a lateral distance of 165 m (541 feet) and a depth of investigation of 33 m (108 feet) for each image. The design for Phase II was to use 56 electrodes at both 3-m spacing (9.8 feet) and 1-m spacing (3.3 feet). This spacing allowed for the same 1.5-m resolution data along three lines as in Phase I, but also allowed for data collection at 0.5-m (1.6 feet) resolution for the lateral distance of 55 m (180 feet) and a depth of investigation of 11 m (36 feet) for three separate lines. The spacing is dependent upon balancing the depth of investigation with how much resolution is needed.

Each ERI line was placed using field measuring tapes to 165 m (541 feet) or 55 m (180 feet). For each line, 56 stainless steel stakes were inserted into the soil approximately 1 foot deep oriented in a straight line. The resistivity cable was laid out and each electrode on the cable was connected to each stake. The cables were connected to the instrumentation once the line was laid out. A generator and an AGI 12-volt power supply were used to power the instrument. Electrical testing was ready to start after transects were set up.

Tests were run on the instrument and cable to ensure each electrode was properly connected to each stake and that the instrument is running properly. Contact resistance tests were

conducted to ensure the circuits were complete. Electrodes with contact resistance greater than 2,000 ohms fail the test and those stakes were either pushed deeper in the soil to help create a better contact with the soil, or an electrically conductive fluid like salt water was poured around the stake to improve contact between the stake and underlying soil. Lower contact resistance indicates better contact with subsurface material, increasing signal strength and improving better data quality and accuracy. With the high soil moisture at the site during the surveys, no extra fluids were required to obtain good electrode contact. ERI data collection began after tests were concluded.

The collected data were evaluated for data quality prior to departing the field. In the laboratory, field electrical data were paired with topographic data and processes to determine 2D resistivity surveys beneath the electrode lines. Data from individual depth horizons were extracted from individual datasets and interpolated to generate depth slices of the site data to provide map views of the site electrical structure. Both 2D vertical and horizontal data were visualized using RockWorks software.

4.1.3 Soil Sampling

Soil sampling was conducted using a field kit, a list of criteria to be met, and evenly proportioned between the three sites. The soil sampling equipment used was an AMS Basic Soil Sampling Kit which included of a 3 ¼" hand auger tool. The samples were collected to a depth of 0.1 m (4 inches). Samples were placed in zip-lock baggies and stored in a cooler until the soil analyses were conducted. The locations for sampling were based on a few criteria: samples were collected at 0.25 m (9.8 inches) away from an ERI electrode to improve the fit between both the soil sampling and modeled ERI sets of bulk resistivity data. The remaining criteria were chosen on a field-by-field basis. Field 5a consisted of 10 samples correlating to distances along transect MTJ101 (Figure 6) and an attempt to sample across a known soil contact. Field 12 consisted of 11 samples, three of which are in the unapplied area of the field, correlating to distances along the

transect MTJ105 (Figure 7). Field 1 consisted of 10 samples, one of which is in the unapplied area of the field that correlate to distances along the transect MTJ111 (Figure 8). After collection, the soil samples were submitted for analysis.

Soil samples were analyzed for the chemistry of the soil solids and grain size of the samples by the University of Arkansas Soil Testing and Research Laboratory using the Mehlich-3 extraction method and sieve analysis (Mehlich, 1984). The Mehlich-3 extraction method provided results for the following constituents for the soil solids: pH, phosphorus (P), potassium (K), calcium (Ca), magnesium (Mg), sodium (Na), sulfate (S), iron (Fe), manganese (Mn), copper (Cu), zinc (Zn), and boron (B).

Soil samples were analyzed for the chemistry of the soil fluids by Oklahoma State University's Soil, Water and Forage Analytical Laboratory using a 1:1 soil-water extraction method as part of a soil salinity management test (Klute, 1986; U.S. Salinity Laboratory Staff, 1954). The 1:1 soil-water extraction method provided the following constituents for the soil fluids: pH, K, Ca, Na, Mg, electrical conductivity (EC), total soluble salts (TSS), potassium adsorption ratio (PAR), sodium adsorption ratio (SAR), exchangeable potassium percent (EPP), and exchangeable sodium percent (ESP). OSU also conducted tests for Total Nitrogen (TN), Total Carbon (TC), and Organic Matter (OM).

The OSU School of Geology conducted isotopic ratio mass spectrometry (IRMS) analysis for nitrogen isotope ratios of the soil samples. The IRMS analysis provided isotopic composition of the soil, which was cross-referenced with that of known isotopic values for swine lagoon effluent. Samples were hand-crushed into a powered, placed into tin capsules, weighed, and formed into spheres before being combusted by an Elemental Analyzer (EA). The EA converted the samples to N_2 gas and passed them through the IRMS where the isotope ratios were measured. Reference material (IAEA-34 and USGS-40), blank tins, and doubles of each sample

were run to ensure accuracy of the machine. The resulting data then underwent correction procedures using values of the reference samples (De Groot, 2004).

4.2 Site Specific Methods

In the following sub-sections, the field methods applied at each site utilized in the study are discribed. Three sites are described for both ERI and soil data collection.

4.2.1 Field 5a

In December 2014, seven ERI transects (MTJ01 – MTJ07) were collected at Field 5a (Figure 3). Three transects ran approximately east-west, while the other four transects ran approximately north-south. Transects were 165 m long and with 3 m spacing to share a similar depth of investigation. Transect MTJ01 was the sole transect to cross Big Creek (Figure 16). The transects MTJ02 and MTJ03 were oriented at an angle to MTJ01 but both shared the east-west trend. MTJ04 and MTJ05 were two of four transects that ran north-south and were paired to create one long transect. These transects ran roughly parallel to the stream and the fence line, and crossed the three east-west trending transects. MTJ06 and MTJ07 were very similar to MTJ04 and MTJ05. They also ran parallel to the stream and fence line, and crossed the three east-west trending transects, but the pair of transects sat approximately 75 m to the east of MTJ04 and MTJ05. Together, these datasets allowed coverage of Field 5a to evaluate the geologic context of the area.

In March 2015, two ERI transects (MTJ101 & MTJ102) were collected at Field 5a (Figure 3). The two transects were in the same orientation as some surveys in from December, approximately north-south and parallel to the stream. The transects were collinear, sharing similar stake locations and both sat atop the MTJ106 and MTJ107 transects which were run during December at this site. MTJ101 was 165 m long with 3 m spacing to share the same depth of investigation as the previous surveys taken on Field 5a. MTJ102 was 55 m long with 1 m spacing

for a higher resolution of the same area as MTJ101. Soil sample locations for the background site (Field 5a) were chosen based on the Phase I ERI results of MTJ106/MTJ107. The Phase I data indicated a possible change in soil characteristics from a thin and rocky soil in the northern part of the field to a thicker soil in the southern part of the field. When conducting the statistical analysis on the data, this change in soil characteristics was used to separate the data into two groups. The sample locations for this site were selected in order to capture the possible soil profile change. The samples correlate to distances along MTJ101 (Figure 6). The separation of the soil samples into the thin, rocky northern half and the thicker southern half was split in the middle at the 82.5 m mark. Five samples fall in the northern half (0.0 – 82.5 m) and five samples fall in the southern half (82.5 – 165 m).

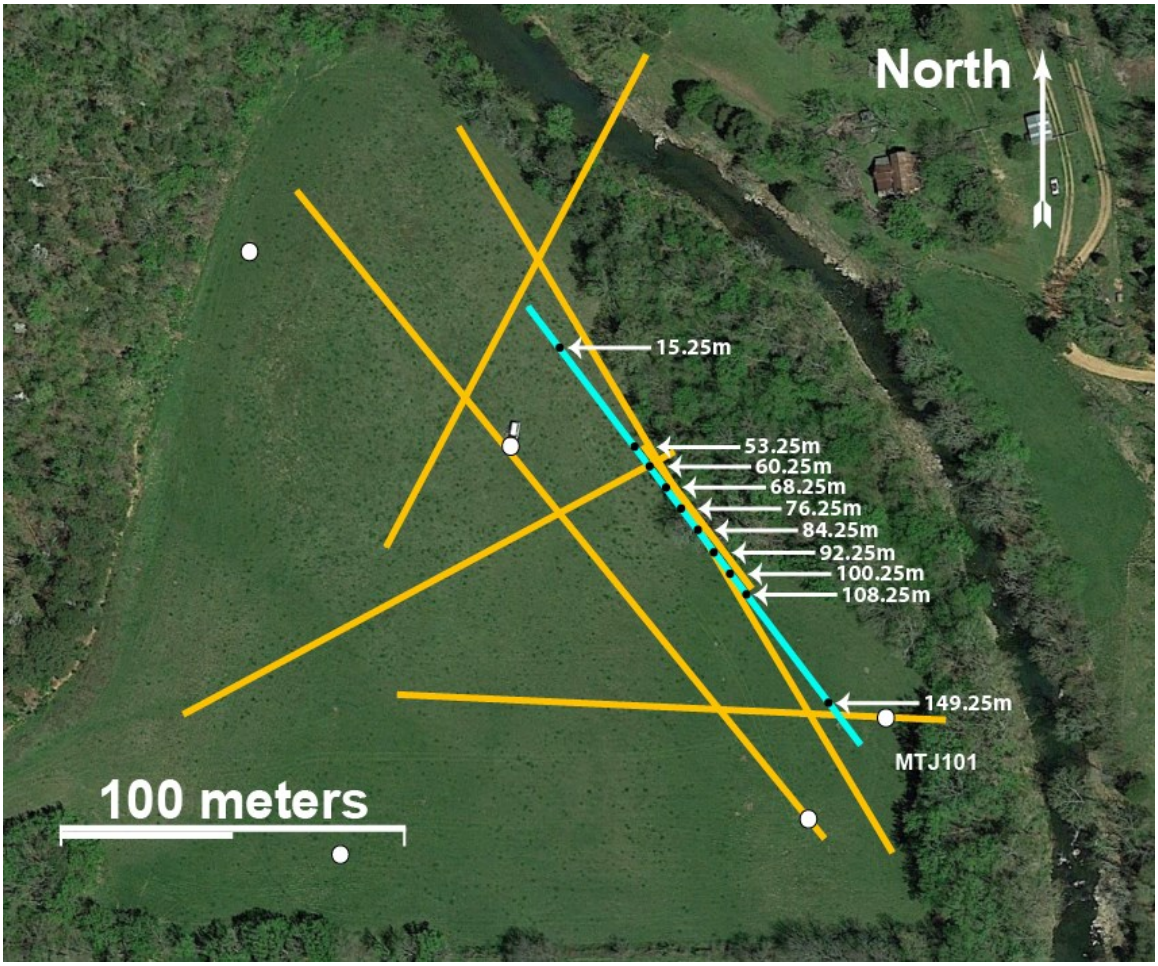

Figure 6 – Black dots represent soil sample locations along transect MTJ101 (blue line) in Field 5a (background site). Yellow lines represent other ERI lines collected at site.

4.2.2 Field 12

In December 2014, five ERI transects were collected from Field 12 (MTJ08-MTJ12) (Figure 4). Three of transects ran approximately east-west, while the other two transects ran north-south. Transects were 165 m long with 3 m spacing to share a similar depth of investigation. Transects MTJ08 and MTJ09 ran parallel to each other and nearly parallel to Big Creek, covering almost the entire length of the field. Transects MTJ10, MTJ11, and MTJ12 ran perpendicular to MTJ08 and MTJ09. All three were parallel to each other and the fence line.

These three ran north-south and were separated from each other by approximately 40 m. This set of transects covered a sufficient area of the field to evaluate the geologic objectives and covered the boundary between the unapplied edge of the field and application zone in the center of the field.

In March 2015, three ERI transects (MTJ104 - MTJ106) were collected at Field 12 (Figure 4). Two transects were in the same orientation as the surveys in December, approximately east-west and perpendicular to the stream. The transects were collinear, sharing similar stake locations. MTJ105 was 165 m long with 3 m spacing to share the same depth of investigation as the previous surveys taken on Field 12. MTJ104 was 55 m long with 1 m spacing for a higher resolution of the same area as MTJ105. These two were approximately 40 m to the north of MTJ12 and both started at the edge of the field nearest the stream. The third transect shared the north-south orientation of transects MTJ08 & MTJ09 and was collected as part of a northern extension to MTJ08. MTJ106 was 165 m long with 3 m spacing to share the same depth of investigation as the other surveys on Field 12. These surveys examined the northern edge of the field (the lowest corner of the field), and increased the area of investigation. Locations of the soil samples for the applied sites (Field 12 and 1), samples were collected in both the application zone and the unapplied edge of the field (33 m, or 100 feet, from edge of field). The sample locations of Field 12 were denser nearest to the edge of the application zone to try and determine if the boundary between application zone and the unapplied edge of the field can be visualized and paired with the ERI data consistently. The samples correlate to distances along MTJ105 (Figure 7).

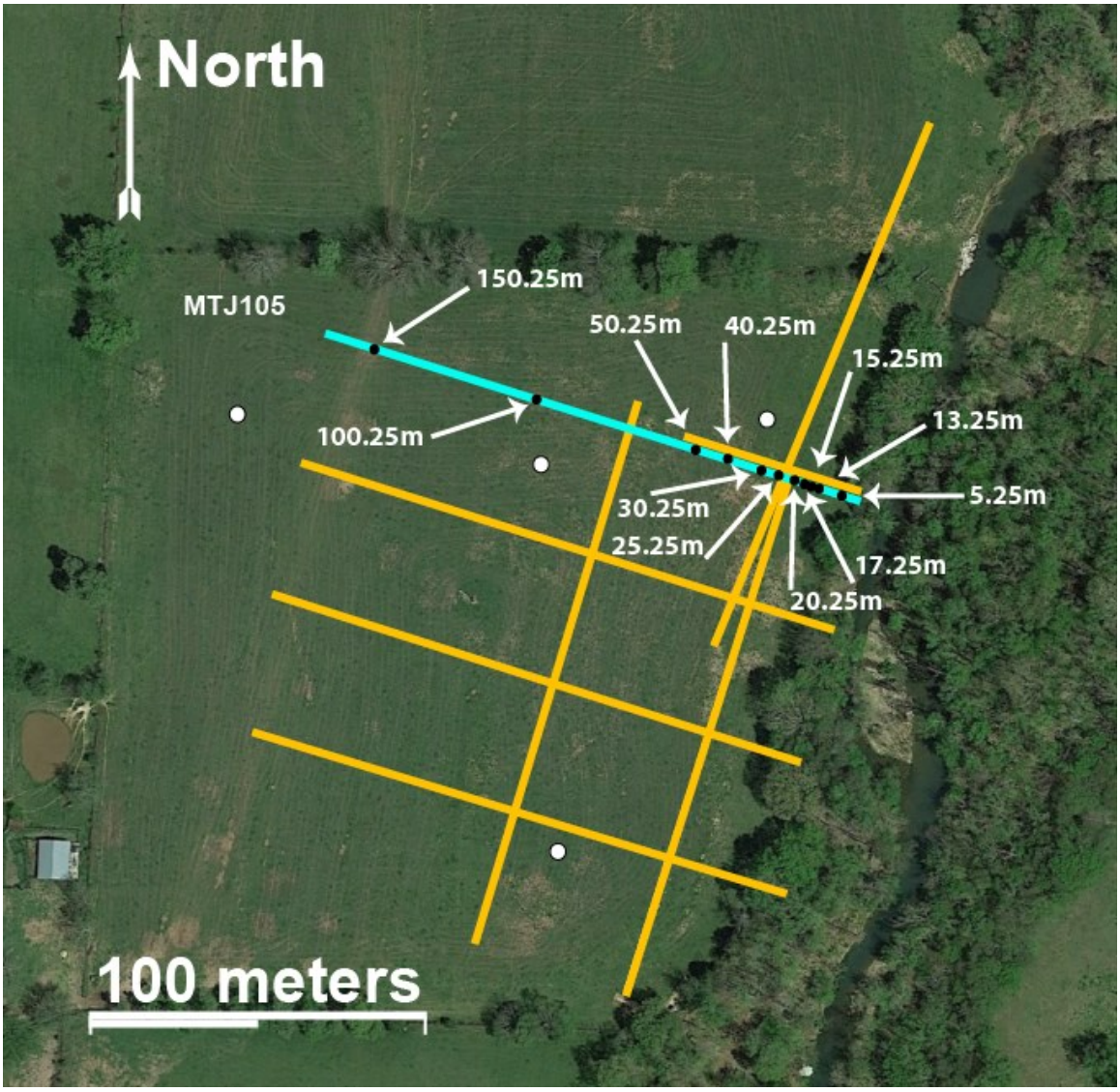

Figure 7 – Black dots represent soil sample locations along transect MTJ105 (blue line) on Field 12 (application site). Yellow lines represent other ERI lines collected at this site.

4.2.3 Field 1

In March 2015, two ERI transects (MTJ111 & MTJ112) were collected at Field 1 (Figure 5). The two transects are collinear and are oriented north-south. MTJ111 was 165 m long with 3 m spacing so as to share the same depth of investigation as the previous surveys taken on the other fields. MTJ112 was 55 m long with 1 m spacing for a higher resolution of the same area as

MTJ111. For the applied sites (Field 12 and 1), samples were collected in both the application zone and the unapplied edge of the field (100 feet from edge of field). The sample locations of Field 12 were denser nearest to the edge of the application area to try and determine if the boundary can be visualized and paired with the ERI data consistently. The sample locations of Field 1 were denser in the small gully in the center of the line but also attempted to determine if there is a difference in the application zone and the unapplied edge of the field. The samples correlate to distances along MTJ111 (Figure 8).

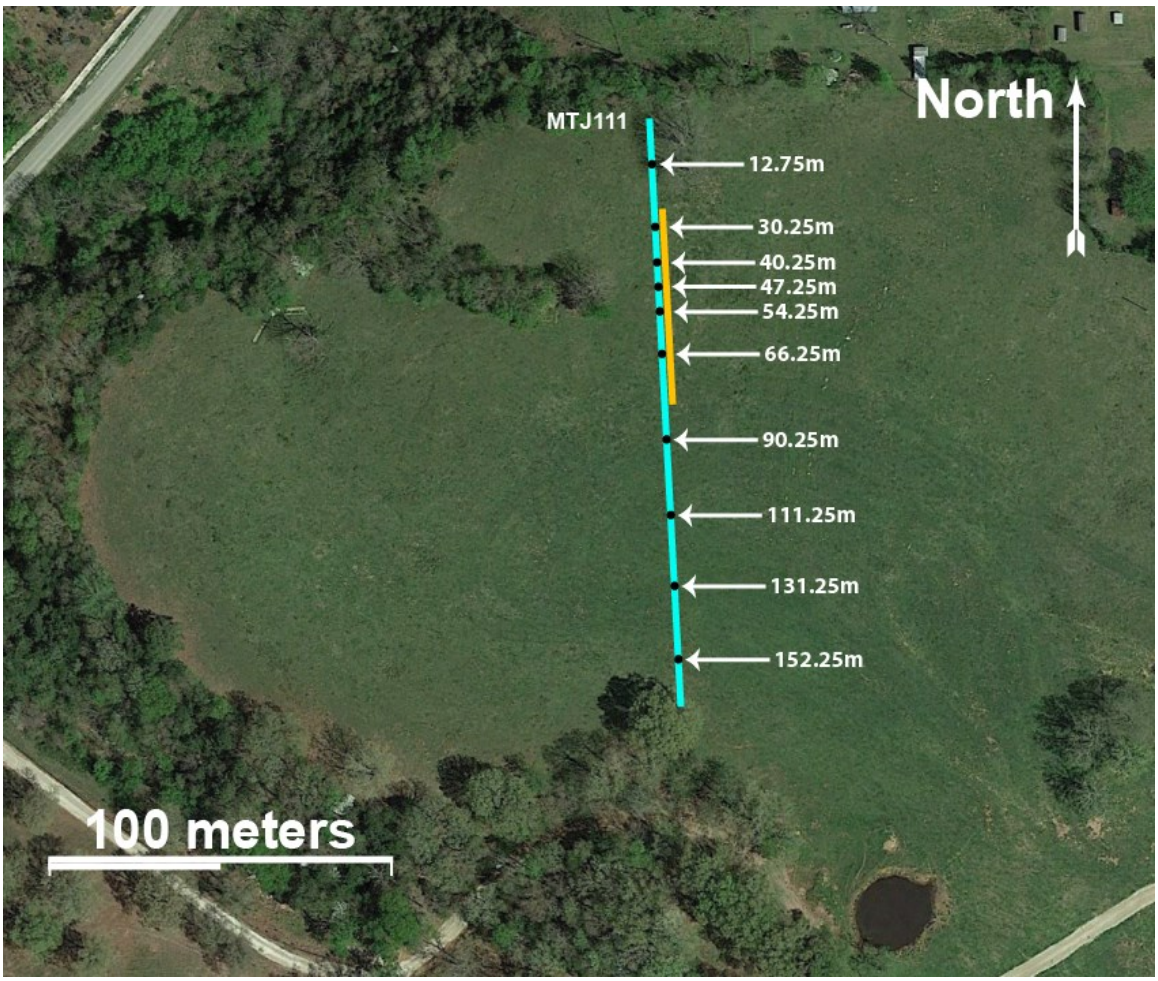

Figure 8 – Black dots represent soil sample locations along transect MTJ111 (blue line) on Field 1 (recent application site). Yellow line represents other ERI line collected at this site.

4.3 Field Data Analysis

During previous work to install monitoring wells by the University of Arkansas, soils were hand-augured until hitting a surface hard enough to prevent further penetration (depth of refusal). These depths were evaluated along with the ERI surveys to produce a distributed understanding of the soil depth and thickness across the sites. The epikarst thickness was found using the ERI surveys based on the use of a strong vertical resistivity gradient to delineate weathered epikarst from competent bedrock. Electrically conductive features can be displayed as pathways within the soil and epikarst (Bolyard, 2007). Resistive electrical layers are interpreted as the limestone bedrock at depth on each site. Linear electrically conductive pathways through the bedrock are interpreted as potential joints or faults. Electrically conductive zones are interpreted as potential dissolution or weathered portions of the bedrock.

Statistical analysis was run on the ERI data to determine if statistically significant differences existed between the soil ERI data between the three fields. Data were selected from the upper line of each dataset where soil samples were collected. The data were averaged to smooth out variability using a five point moving average. A two-tailed t-test was used to determine significance and alpha was assumed to be 0.05, or the 95% confidence interval. The data were also tested for the three sites to evaluate if the 0.5 m resolution data were statistically different from the 1.5 m resolution datasets.

Statistical analysis was run on the soil sample test results to determine if significant variations existed in the parameters between the three fields (see Appendix 6 for data). A two-tailed t-test was used to determine significance and alpha was assumed to be 0.05, or the 95% confidence interval. A margin of error was calculated as $0.98/\sqrt{n}$ (Johnson and Bhattacharyya, 2006), where n is the number of samples. These analyses were performed to compare the background data against the applied sites and to compare the recently applied site to the other two sites.

Correlation between the datasets was analyzed by comparing the two soil types sampled in the background field against the soil analysis data. Correlation for the applied sites was performed by comparing the areas inside the application zone against the corresponding ERI data. Goodness of fit estimates for the relationships were calculated using Excel. The goodness of fit analyses were separated into one of four categories: none or very weak relationship ($r^2 < 0.1$), weak relationship ($0.1 < r^2 < 0.3$), moderate relationship ($0.3 < r^2 < 0.5$), and strong relationship ($0.5 < r^2$).

4.4 Numerical Modeling

The following sub-sections were the methods used to create a numerical model. We generated a model which simulated swine lagoon effluent application and precipitation events.

4.4.1 Model Characteristics

Reactive transport modeling was conducted to simulate a swine lagoon effluent application to a site. The model was generated using TOUGHREACT model with the PetraSim5 interface. A vertical 1-D model of a 3-m thick soil column was designed and divided into 30 horizontally stacked cells, each 10 cm in thickness (Figure 9). Six simulated materials (Table 2) were created within the program: ATMOS, 1LOAM, 2LOAM, 3SCLL, 4SCLL, 5fSLO, 6GfSL, and ROCK1. Because our soil samples were collected only to a depth of 10 cm (4 inches), the materials were simulated based on literature values (Ferguson, 1920; Fowlkes et al., 1988). ATMOS is representative of atmospheric conditions and the top most cell (cell 30) from 0 – 10 cm. 1LOAM and 2LOAM are representative of soil loams from 10 – 20 cm (cell 29) and 20 – 40 cm (cells 28 – 27) in depth. 3SCLL and 4SCLL are representative of sandy clay loam soils from 40 – 60 cm (cells 26 – 25) and 60 – 100 cm (cells 24 – 20) in depth. 5fSLO simulates a fine sandy soil from 100 – 140 cm (cells 20 – 16) in depth. 6GfSL models a gravelly fine sandy loam from 140 – 250 cm (cells 16 – 5) in depth. ROCK1 is representative of the Boone Limestone bedrock

from 250 – 300 cm (cells 5 – 1), the base of the model. Because we did not have confirmation on saturation, an artificial water table was set at 2-m deep and had decreasing saturation with increasing height above the water table as these were arbitrary values divided by the number of cells left to be filled (Figure 10). The initial chemistry for the soil column in the model was based on values from the field soil sample analysis (one cell from top) and the water quality database for the Buffalo National River (lowest 28 cells) (National Park Service, 2016). Sorption parameters (density and K_D) were determined from National Resources Conservation Service (2008) and Whetstone Associates, Inc. (2011), respectively. Wet Heat Conductivity and Specific Heat were set to 2 W/(m*K) and 1000 J/(kg*K), respectively. Flow in the model follows the van Genuchten-Mualem (IRP=7) equation for relative permeability and the van Genuchten Function (ICP=7) equation for capillary pressure.

Table 2 – Material Assignments

Cell Assignment	**Density kg/m^3**	**Porosity**	**Permeability mD**
ATMOS	1.225	0.99	1.01E+11
1LOAM	1500	0.45	243
2LOAM	1500	0.45	243
3SCLL	1500	0.42	212
4SCLL	1500	0.42	212
5fSLO	1550	0.44	1013
6GfSL	1570	0.44	2330
ROCK1	2500	0.12	101

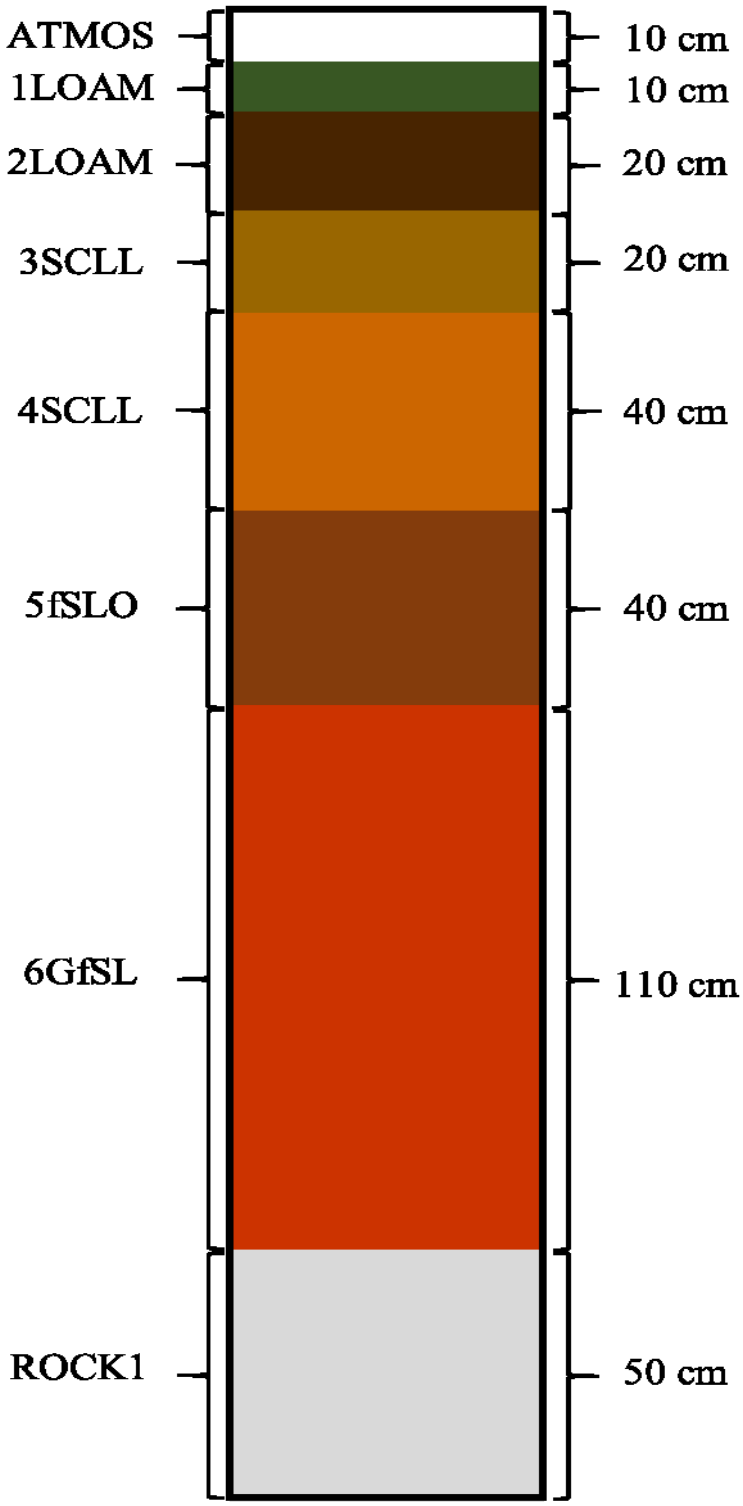

Figure 9 – Vertical 1-D model domain divided into 30 horizontally stacked cells (10 cm in thickness each) with model cell assignments for lithologic parameters.

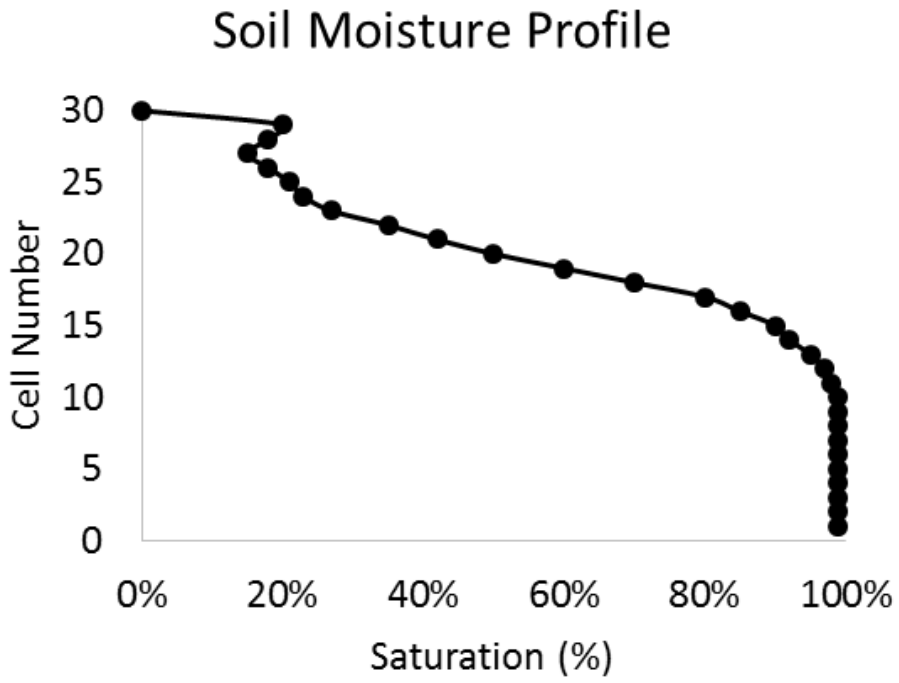

Figure 10 – Starting model soil moisture profile (initial conditions set for simulation).

4.4.2 Simulated Application and Rainfall

The initial chemistry (Table 3) for the simulated swine lagoon effluent application was based on values from a slurry sample analysis (Big Creek Research and Extension Team, 2013). The simulated application flux was based on the field application data for Field 12 (Big Creek Research and Extension Team, 2013). Simulated precipitation events were determined from the Rainfall Frequency Atlas of the United States (Hershfield, 1963) for a 1-year, 24-hour storm event and from the Annual Climatological Report for North Little Rock, Arkansas (National Weather Service, 2016).

Table 3 - Initial chemistry of model.

Constituent	Effluent Application Concentration (mol)	Topsoil Concentration (mol)	Subsurface Concentration (mol)	Rainfall Concentration (mol)
H	1.00E-07	1.00E-07	1.00E-07	1.00E-07
H_2O	1.00	1.00	1.00	1.00
Ca	5.62E-03	4.23E-02	1.07E-03	5.44E-05
Fe	7.00E-04	3.21E-03	1.02E-07	1.79E-05
K	7.30E-03	2.58E-03	2.99E-05	7.93E-05
Mg	2.48E-03	4.43E-03	9.30E-05	1.36E-04
Mn	5.63E-05	3.66E-03	6.37E-08	1.82E-05
S	8.41E-04	9.00E-04	1.88E-04	3.75E-05
Zn	7.93E-05	7.00E-05	4.39E-08	1.57E-05
Cu	9.23E-06	3.00E-05	1.42E-09	1.57E-05

The model period was one year (Table 4). The rate for application was determined from the application volume spread out over one simulated day. Immediately following application, we simulated the first of 13, 1-yr, 24-hr rainfall events. The maximum probability for a single 1-yr, 24-hr rainfall event for this site was 15.0%, however, the model does not account for runoff so this entire volume is pushed through the model. After every 24-hr rainfall event, we simulated 27 days of no rainfall. The total of the 13 events sums to the average annual precipitation for our site. This provided an end member scenario of large rain events affecting effluent transport.

Table 4 – Simulation Timing

Simulation Name	Number of simulations	Precipitation kg/s	Run-Time days	Run-Time seconds	Timestep seconds
Application	1	2.63E-06	1	8.64E+04	10
Rainfall	13	5.00E-05	1	8.64E+04	10
No Rainfall	13	2.00E-10	27	2.33E+06	10

CHAPTER 5

5.0 RESULTS

Field work in Mt Judea consisted of two trips for eight field days in total to collect ER and soil data. Lab work included processing and interpreting ER and soil data. Results include the processed and corrected GPS data, processed ERI data, detailing soil, epikarst, and bedrock features, and soil analysis. Raw data can be found in the electronic report appendices.

5.1 GPS Data Analysis

The location data collected using the GPS system was processed to evaluate the position of the ERI datasets and site topography. The base data were submitted to the Online Positioning User Service (OPUS), which is operated by the National Oceanic and Atmospheric Administration (NOAA), and the products are the corrected values for easting, northing, and elevation of the base positions in UTM coordinates. These were then applied to the datasets to obtain centimeter-scale accuracy for the topography in the ERI datasets.

5.2 ERI Data Structure

For the processed ERI datasets, it was found that the average root mean square error (RMSE) between the resistivity model and the field apparent resistivity data was 3.16% for Field 5a and 3.34% for Field 12. For Phase II, the processed ERI datasets averaged a RMSE of 3.95% for Field 5a, 3.35% for Field 12, and 6.18% for Field 1. The lower the RMSE percentage, the better the relationship between the collected apparent resistivity data and the calculated

subsurface resistivity model, with values above 15% being considered poor. The range of RMSE for the site was 3.0%-7.8% overall, with an average RMSE of 4.0%. The data quality for the site is good as there were no utilities or other anthropogenic features and the soil was moist at the time of data collection providing good contact with the ground.

The resistivity values for the sites range from *very electrically conductive* to *highly resistive* (Figure 11). The terms used to indicate a specific range are indicated in *italics* for clarity. Electrically conductive areas generally include the shallow portions of the images, with strong resistors at depth. The resistivity measurements for Field 5a range from 1 - $6x10^5$ Ohm-meters with a median value of 1500 Ohm-meters. The resistivities for Field 12 range from 20-$6x10^5$ Ohm-meters with a median value of 1600 Ohm-meters. The resistivities for Field 1 range from 4-$1x10^6$ Ohm-meters with a median value of 1300 Ohm-meters.

The interpretation scale (site specific interpretation) for the resistivity values of the images follow those electrical features:

- **Above 1000 Ohm-meters** generally represent unweathered bedrock with fresh groundwater and will be referred to as *highly resistive*.
- **Between 500 to 1000 Ohm-meters** represent weathered bedrock with fresh groundwater and will be referred to as *very resistive*.
- **Between 150 and 500 Ohm-meters** typically represent significantly weathered bedrock material with fresh groundwater and will be referred to as *resistive*.
- **Less than 150 Ohm-meters** but greater than 50 Ohm-meters are interpreted as soil and/or possible electrically conductive fluids and referred to as *electrically conductive*.
- **Below 50 Ohm-meters** represent fine soils, microbial mass, and/or electrically conductive fluids and referred to as *very electrically conductive*.

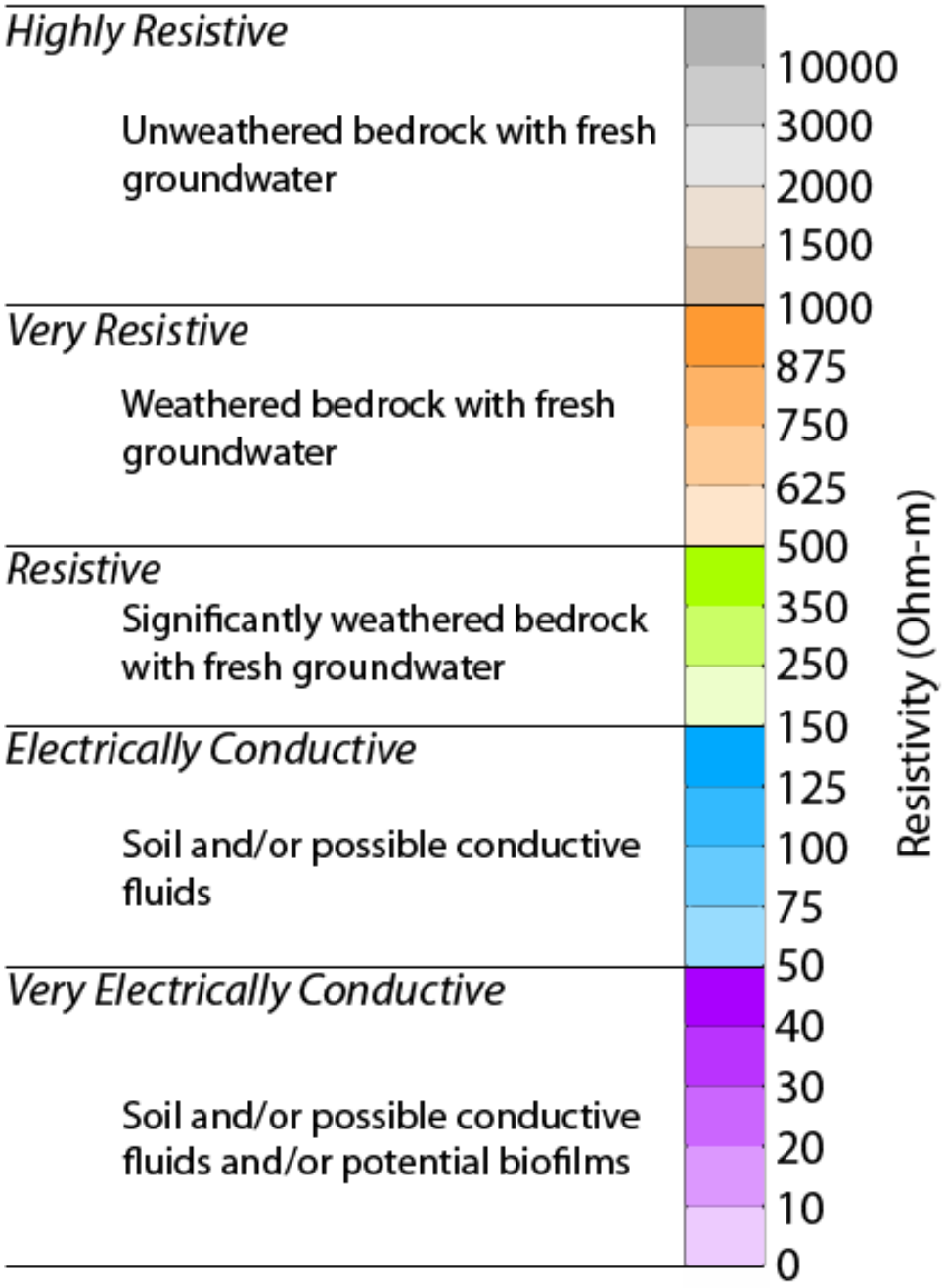

Figure 11 – Resistivity scale for Mount Judea ERI datasets. Cool colors are used to indicate more electrically conductive subsurface locations and warm colors are used to indicate more resistive locations.

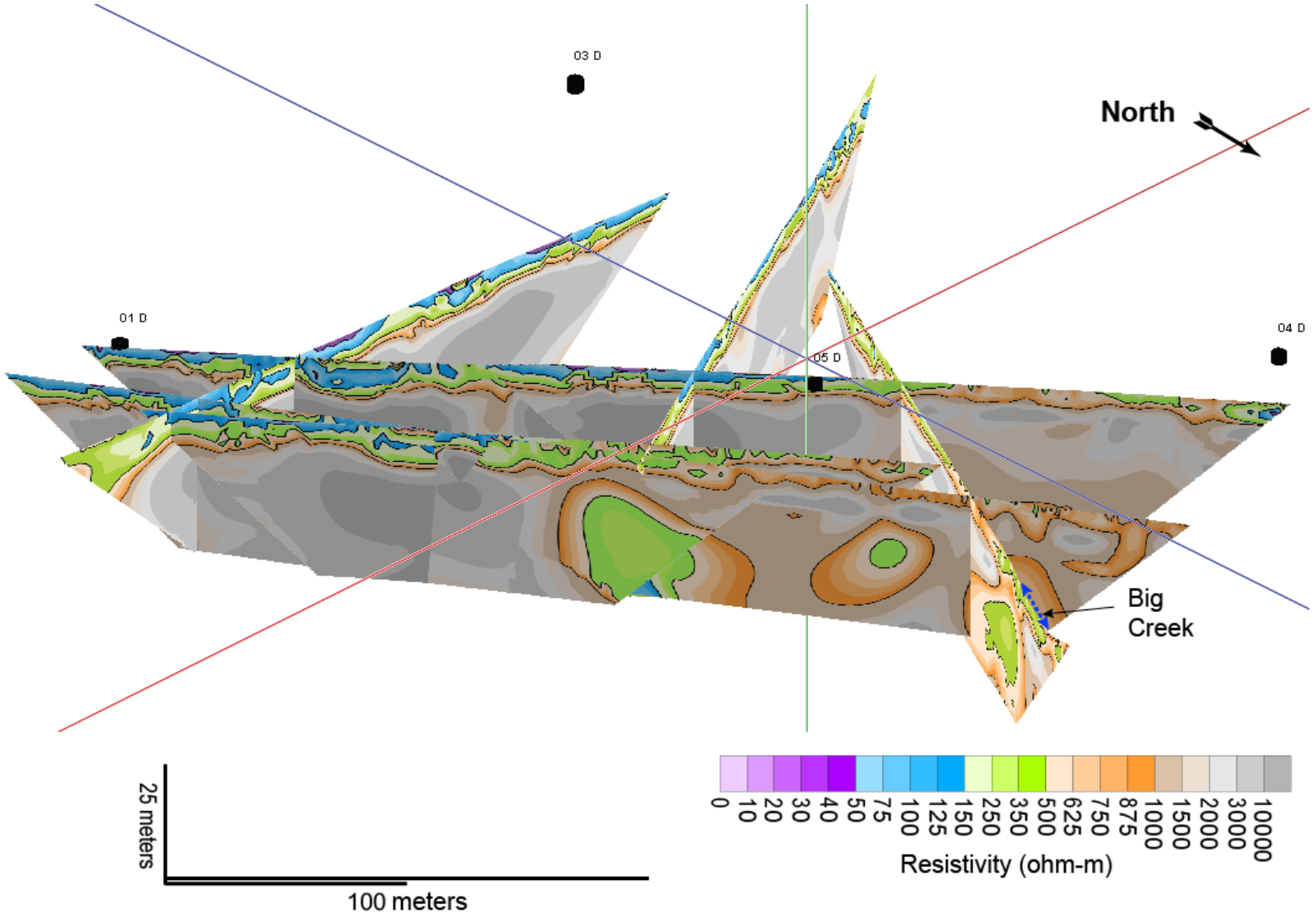

Figure 12 – Field 5a (background site) view from northeast corner of field (from Big Creek toward the field).

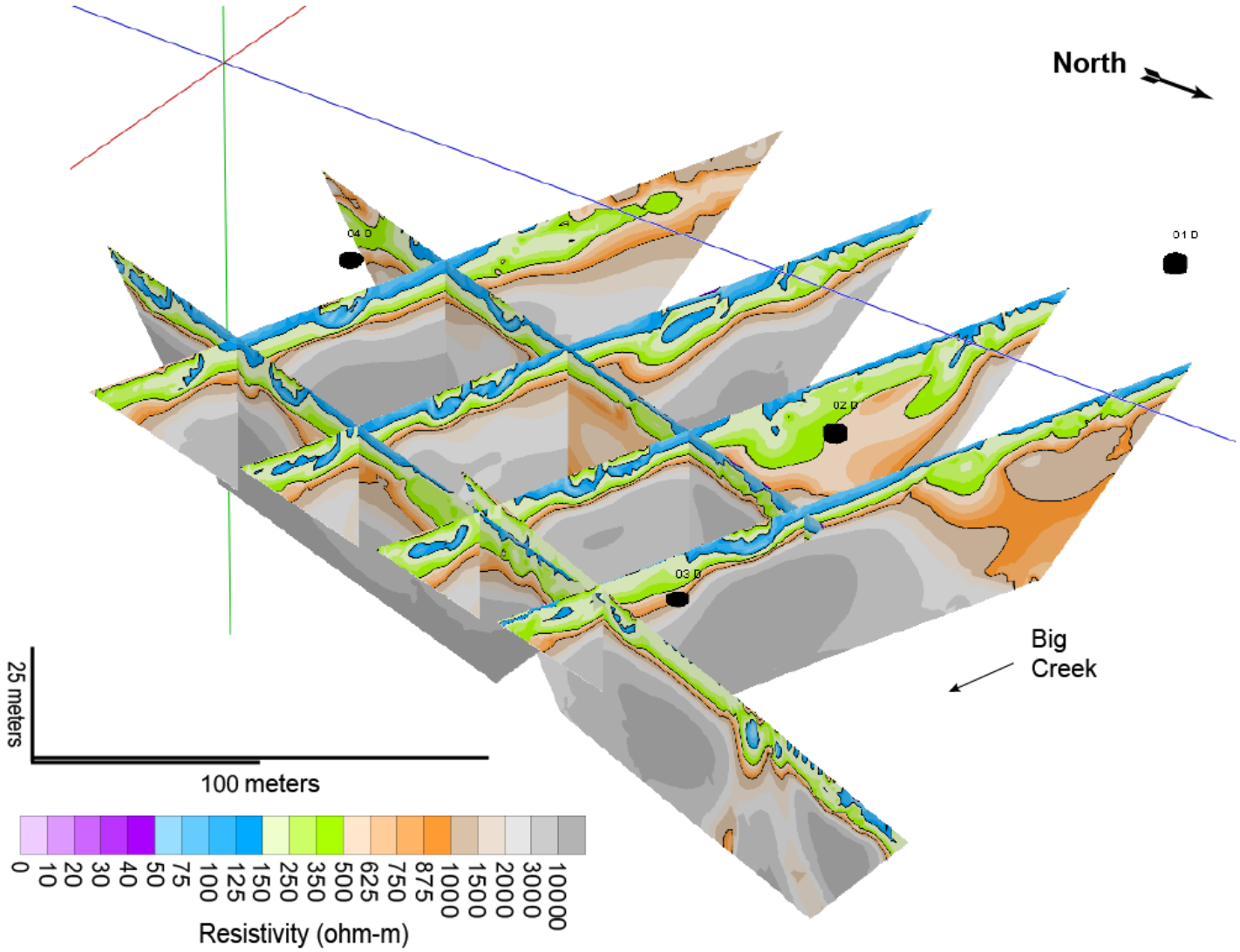

Figure 13 – Field 12 (application site) view from northeast corner of field (from Big Creek toward the field).

5.2.1 Soil Structure

The soil structure analysis consists of soil thickness and soil properties. Soil thicknesses for each site were picked and confirmed through hand dug borings on site which were conducted during previous University of Arkansas work on these fields. These borings were dug to refusal, or where the soil turns to epikarst (significantly weathered bedrock). Soil properties were detailed based on field notes, ERI results, and grain size analysis.

Field 5a is a low-lying grazing area with low relief and an uneven topsoil surface. Field 5a exhibits average soil thicknesses of 0.5 – 4.5 m (1.5 – 14.75 feet). Soil thickness on Field 5a varies throughout, but there is a significant resistivity difference between the *highly* to *very resistive* north and more *electrically conductive* southern portion (Figure 12). There is a broad topographic mound northwest of the center of Field 5a and the soil thickness is thinner to the far north and far west of the field (see Appendix 3). This trend is consistent with the direction to which the alluvium would be deposited nearest to the stream. Soils on transects MTJ06 and MTJ07 (Figure 14A) are those *electrically conductive* features, which thin to near zero soil thickness toward the far north. Grain size analysis (see Appendix 6) indicates Field 5a is a sandy loam to clay loam. Field 5a and Field 12 share some of the soil characteristics.

Field 12 is a low-lying grazing area with low relief and an uneven topsoil surface. Field 12 exhibits similar average soil thicknesses at 0.7 – 4 m (2.25 – 13 feet). Soil thickness on Field 12 is not as variable as Field 5a but there is a *very resistive* portion of the site in the shallow soil area is in the southwest portion of the investigation area (Figure 13). Field 12 is flatter and the soil thins to the west (see Appendix 3). MTJ12 (Figure 15A) shows thinning where the *electrically conductive* features become thicker as the image gets closer to the stream. This trend is consistent with the direction to which the alluvium would be deposited nearest to the stream. Areas where the soil profile is thinner on the images are consistent with the rocky soils which

were encountered when electrodes were placed for data collection. Grain size analysis (see Appendix 6) indicates Field 12 is a sandy loam to clay loam.

Field 1 is a grazing area that sits on a hillside east of the stream. It has low to moderate relative relief and an uneven topsoil surface. Field 1 shows an average soil thickness of 0.5 m (1.5 feet) determined from the ERI surveys of MTJ111 and MTJ112 (Figure 19) and soil sampling but did not have confirmation hand dug borings. This site was not studied extensively enough to determine differences in resistivity that can correlate across the entire field. Field 1 has thinner and rockier soils than either Fields 5a or 12 and gravels present in Field 1 samples with sizes up to 0.05 m (2 inches) across and subsequently removed during soil sampling. Field 1 has a different soil thickness and properties than Fields 5a or 12.

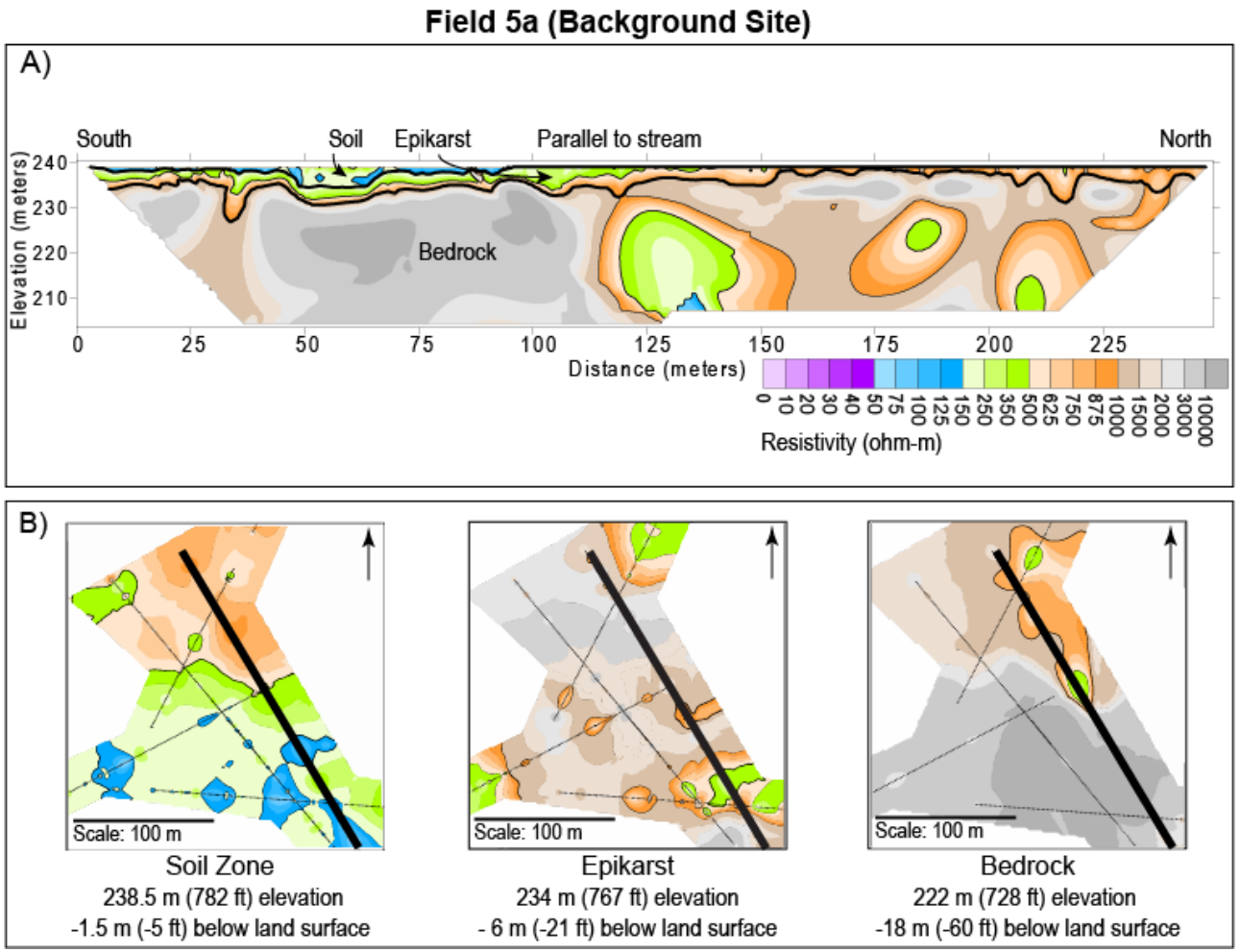

Figure 14 – A) Interpreted Soil-Epikarst boundary and Epikarst-Bedrock boundary for the Field 5a for combined ERI datasets MTJ06 and MTJ07 (background site) cross sections. B) Interpolated 2D depth slices of resistivity at differing elevations illustrating a map view of the subsurface. Heavy black line indicates location of cross section in A).

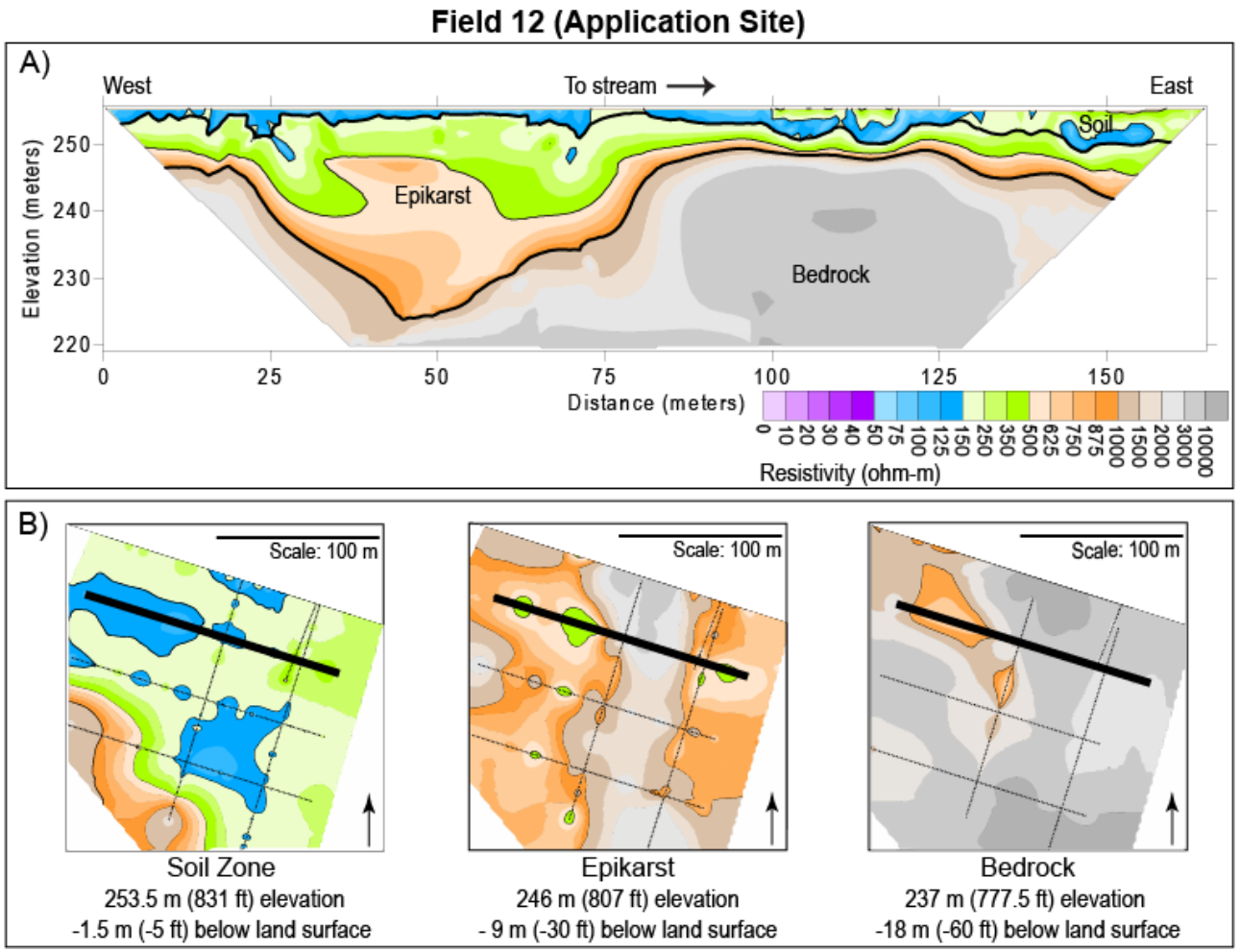

Figure 15 – A) Interpreted Soil-Epikarst boundary and Epikarst-Bedrock boundary for Field 12 for ERI dataset MTJ12 (application site) cross sections. B) Interpolated 2D depth slices of resistivity at differing elevations illustrating a map view of the subsurface. Heavy black line indicates the location of the cross section from A).

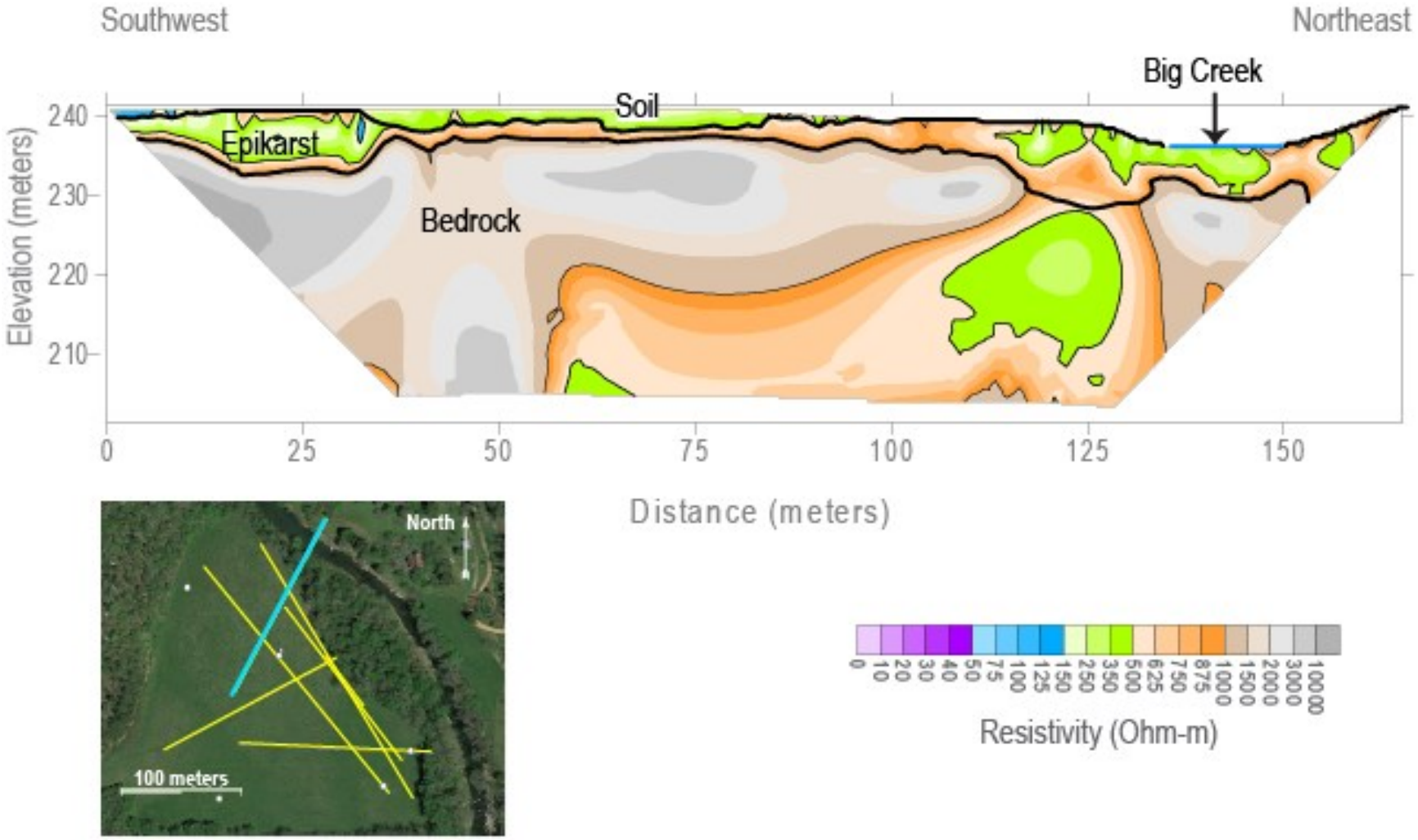

Figure 16 – Field 5a (background site) – Transect MTJ01 with 3 meter spacing.

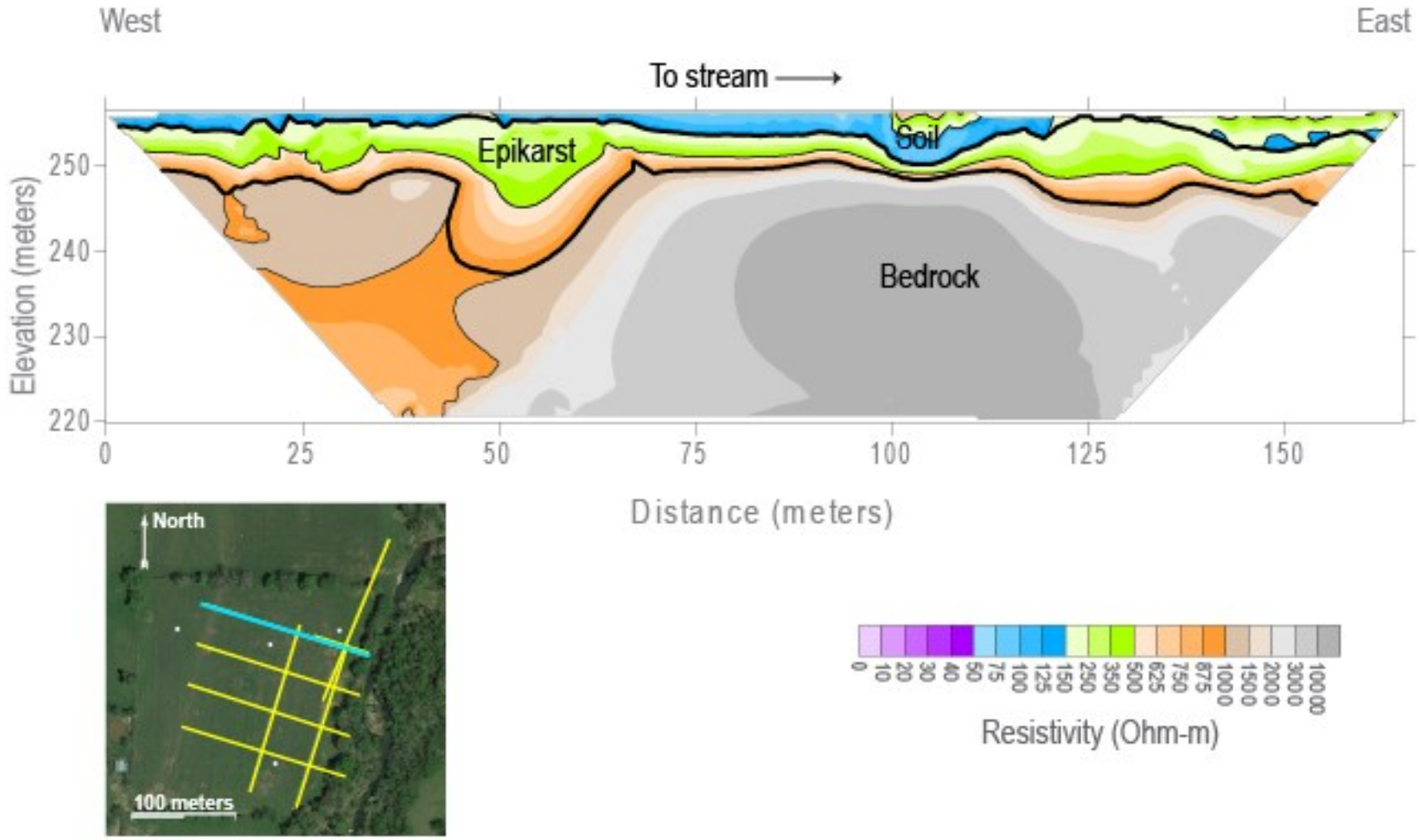

Figure 17 – Field 12 (application site) – Transect MTJ105 with 3 meter spacing.

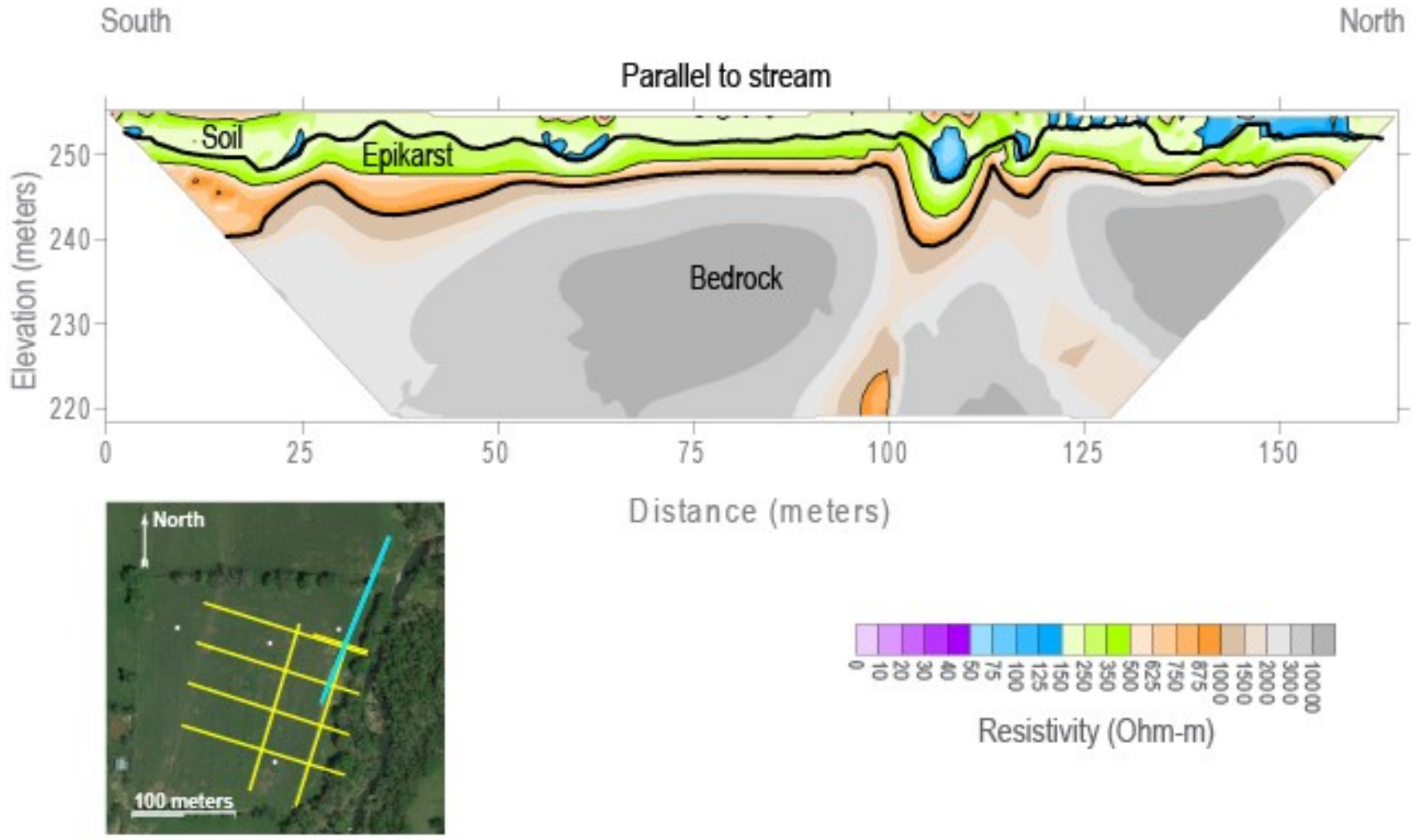

Figure 18 – Field 12 (application site) – Transect MTJ106 with 3 meter spacing.

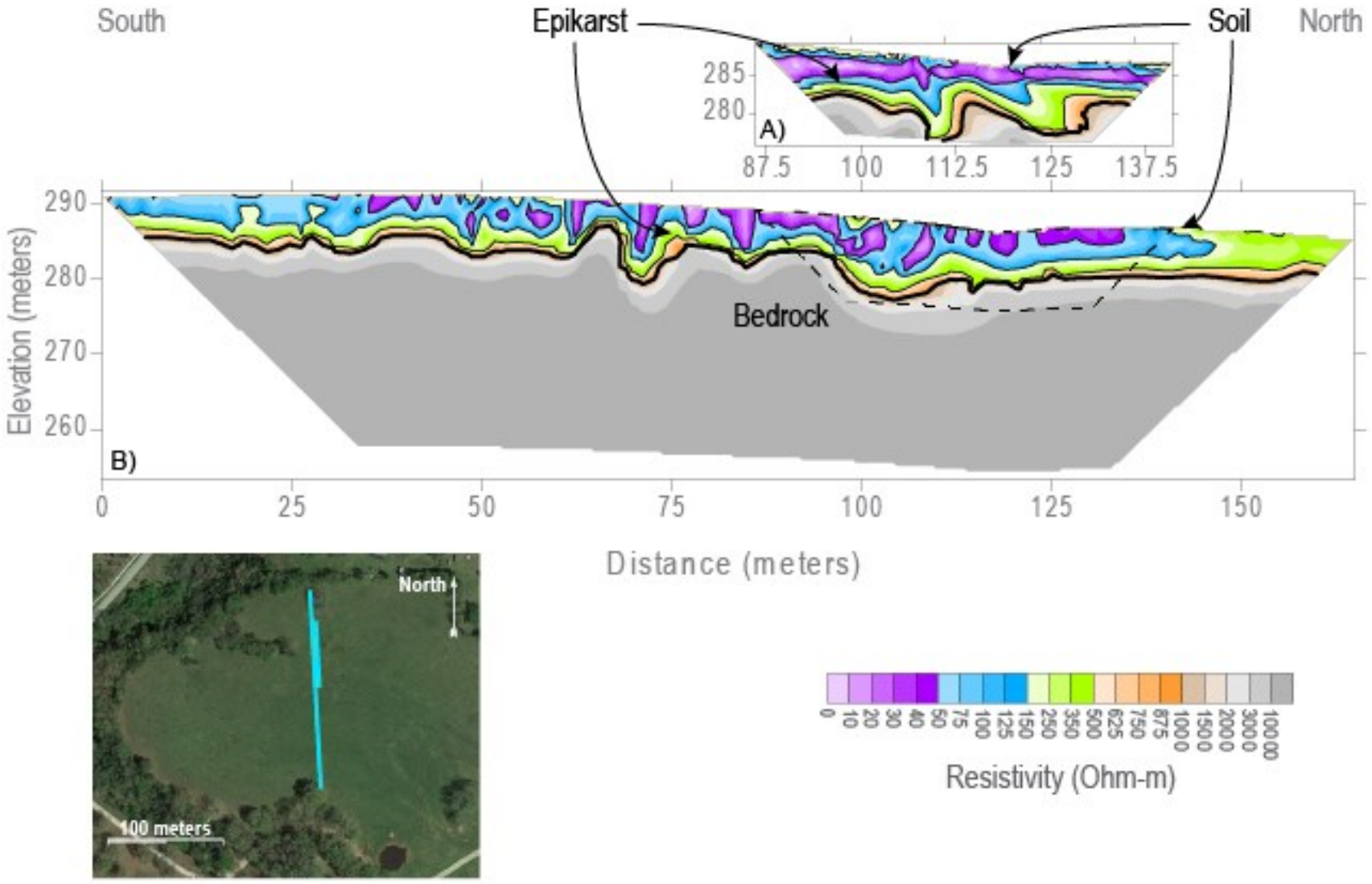

Figure 19 – Field 1 (recent application site) – Transect MTJ111 with 3 meter spacing and Transect MTJ112 with 1 meter spacing.

5.2.2 Epikarst Structure

The epikarst zone consists of the weathering profile of the underlying competent bedrock. Epikarst is visible on Field 5a (Figure 14), Field 12 (Figure 15), and Field 1 (Figure 19) as a more *resistive* to *electrically conductive* region below the base of the soil and above the *highly resistive* competent bedrock zones. No confirmation borings are available to evaluate rock properties in these zones on any of the sites. Because the interpreted base of the epikarst varies from site to site, the threshold for competent rock was quantified at values larger than 1000 Ohm-meters consistent with a strong horizontal resistivity gradient across the images (Figure 12, Figure 13, and Figure 19). The thickness of the epikarst zone is highly variable (thicknesses range from 2 – 23 m or 6.5 – 75.0 feet) throughout each field but averages 4 – 7 m (13-23 feet) thick.

Average epikarst thickness for Field 5a is 4 m (13 feet) and it relatively thin and similarly to the soil zone, thicker in the southern half of the field. At locations where electrically conductive features exist in the bedrock, the epikarst generally appears connected in space with these features (Figure 14 and Figure 16). ERI dataset MTJ01 shows the most variation in epikarst thickness on Field 5a (Figure 16).

Average epikarst thickness for Field 12 is 6 m (20 feet) and the epikarst surface on Field 12 is very irregular in many transects (see Appendix 3). There appears to be a large doline feature (a closed topographic depression caused by dissolution or weathering of underlying rock or soil) within the bedrock on transect MTJ12 that is approximately 61 m (200 feet) across at the top of the feature starting 8 m (26 feet) below the land surface and extends 23 m (75 feet) vertically downward (Figure 15A).

The determined average epikarst thickness for Field 1 is 5 m (16.4 feet). Delineating the top of the epikarst from the soil on Field 1 is different from the other sites as there are no confirmation hand dug borings near the transects and the resulting images show *very electrically conductive* features protruding into the subsurface in irregular vertical structures (Figure 19).

Along the line of soil sampling however, most of the samples encountered the top of epikarst with limestone gravel in the top 6 inches of the site. This implies the soil zone is thin relative to the epikarst.

5.2.3 Bedrock

The Boone Formation is the underlying rock unit across these fields and is considered the bedrock. In many of these cross-sections, the limestone is interpreted as large, *highly resistive* blocks. The values for the more competent limestone are interpreted as those greater than 1000 Ohm-meters. It is evident on all three fields (Fields 5a, 12, and 1) that a *highly resistive* zone interpreted as bedrock is located at depth (Figure 14, Figure 15, and Figure 19, respectively). No confirmation borings are available in the bedrock zones to confirm rock properties, but limestone is present in the streams adjacent to Fields 5a and 12, and a quarry is present near Field 1.

Field 5a is on average electrically resistive and has a thin layer of alluvium at the foot of a steep hill to the west of the field (Figure 14). The majority of the surveys taken in this field display a very large and blocky *highly resistive* bedrock, especially to the southwest corner. Lines MTJ01 and MTJ06 (Figure 16 and Figure 14, respectively) both show that the northern corner of the field is electrically different bedrock than the southern portion of the field (Figure 14B). This zone also has a number of *electrically conductive* features that could be interpreted as karstic zones. The largest of these zones is at 120 m along ERI line MTJ06/07 (Figure 14A).

Field 12 does not have as many *electrically conductive* features at depth as Field 5a, however it does have some possible doline features within the bedrock (Figure 15A). There are also some possible fractures indicated by vertically oriented conductors to the northern section of the field in MTJ105 and MTJ106 (Figure 17 and Figure 18, respectively). The bedrock here appears more competent and blocky than Field 5a but is still appears to be potentially fractured.

Field 1 does not have the same alluvium layer above limestone bedrock as Field 5a and 12, therefore the bedrock boundary is shallower on this site alone. Field 1 does not share the same

fractured characteristics as the other two sites (Figure 19). This site has a very high electrical gradient going from the epikarst zone to the *highly resistant* bedrock.

5.2.4 Site Comparison of ERI Data

A difference can be seen in bulk electrical resistivity values of the three sites. Fields 5a and 12 compare favorably with very similar electrical resistivity values. The resistivities for Field 5a range from 1 – $6x10^5$ Ohm-meters with a median value of 1500 Ohm-meters. The resistivities for Field 12 range from 20 – $6x10^5$ Ohm-meters with a median value of 1600 Ohm-meters. Field 1 is slightly more electrically conductive overall when comparing the three sites. The resistivities for Field 1 range from 4 – $1x10^6$ Ohm-meters with a median value of 1300 Ohm-meters. The values of bulk electrical conductivity (the inverse of electrical resistivity) from the top of the three 165 m long, 1.5 m resolution ERI transects, one from each site, run during Phase II show a difference between the electrical conductivity of the three fields (Figure 20). Field 1 and Field 12 have increases in bulk conductivity occur at around 30 m laterally on the image which would be the boundary of application of manure. In the higher resolution datasets, (55 m long, 0.5 m resolution) the variations between the fields are not as clear. Field 1 still has the most conductive features, but it is similar to a feature on Field 5.

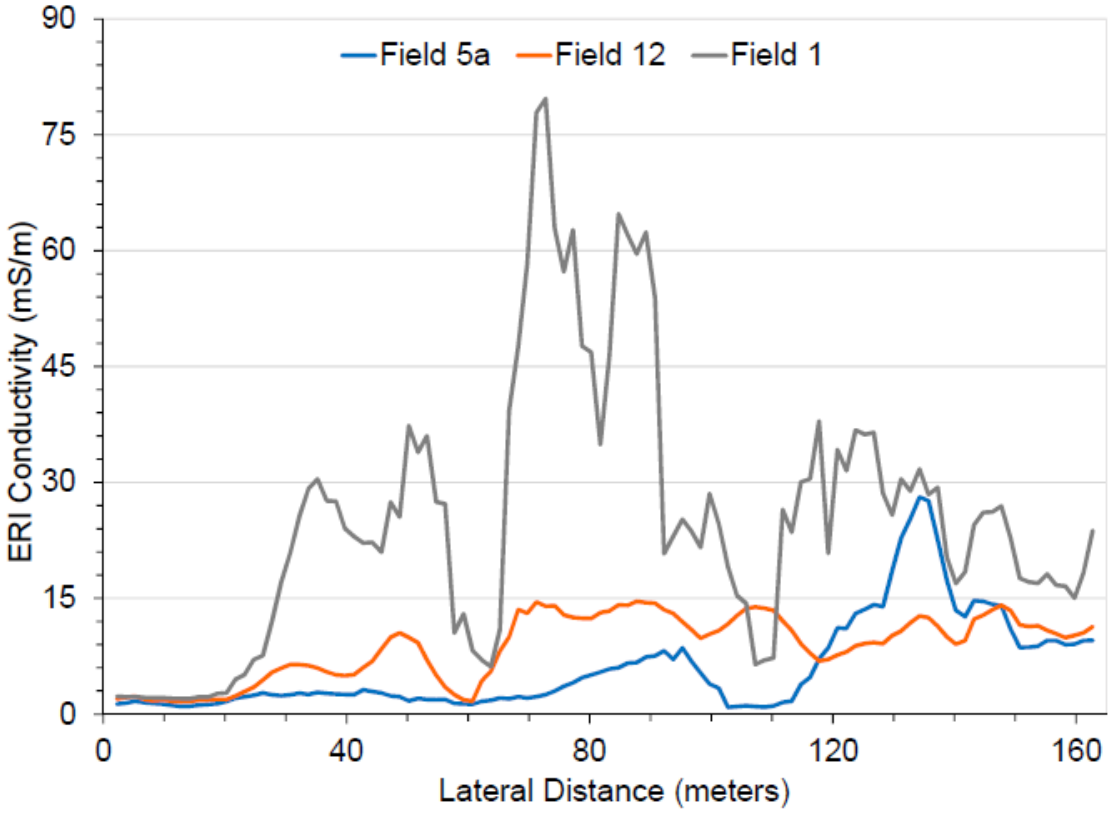

Figure 20 – Electrical conductivity of the top row of data (model cells are 0.25 m thick) from each site during Phase II at 1.5 meter resolution. Data has been smooth with a 5 point moving average to make the plot clearer.

5.3 Soil Analysis

Soil samples were collected along the ERI transects during March 2015 to correlate between geophysical (resistivity data) and the physical and chemical properties of the soil. In sum, 31 soil samples were collected, across the three fields (see Appendix 6). Statistics were run on the results to find if there is any correlation between the fields or between soil types or applied vs unapplied areas.

5.3.1 Soil Testing

To examine all three sites, soil tests were conducted and compared for trends in the data. Averages for all sites of the results of the Mehlich-3 soil test are displayed in Table 5 and averages for all sites of the results of the soil salinity test (1:1 soil-water) are displayed in Table 6 (Full dataset in Appendix 6). Table 7 contains the results of the organics contents for all sites. Field 5a (background site) was found to have lower averages in almost many constituents, but the highest average TC, TN, and OM content. Fields 12 and 1 (application sites) are consistently higher than Field 5a in almost all sample types, but lower in average TC, TN, and OM content. Field 1 is highest in all categories except in calcium and sodium, while it is lowest in TN, TC, and OM values. Field 1 has similar values to Field 12 in both fluid EC and TSS. Statistical analysis was applied to all of the results to determine if there was a statistical difference between sites.

Table 5 – Results for various constituents on each field after Mehlich-3 extraction method (dry method for solids analysis).

Constituents	Field 5a	Field 12	Field 1
pH	5.4	5.7	6.5
P (ppm)	49.3	72.1	83.2
K (ppm)	66.5	100.9	232.1
Ca (ppm)	1283.0	1696.9	1314.8
Na (ppm)	15.1	107.6	15.4
Mg (ppm)	76.7	13.9	129.2
S (ppm)	24.5	28.7	28.6
Fe (ppm)	170.4	179.0	194.6
Mn (ppm)	188.7	201.1	636.4
Cu (ppm)	1.4	1.9	1.6
Zn (ppm)	2.6	4.3	5.0
B (ppm)	0.1	0.1	0.1

5.3.2 Nitrogen Isotopes

To examine all three sites, isotope analysis was conducted and compared for trends in the data. Nitrogen isotope analysis was decided upon for analysis of the soil samples to determine if there was a detectable signature of the applied swine lagoon effluent within any of the soil samples. The δ15N is compared to isotope signatures from other agricultural areas. The data from all 31 samples and their duplicates, ranges from 3.8‰ – 6.6‰ across all three sites. The average is lowest for Field 1 (recent application site) with an average at 4.8‰ (0.5 SD) and a range of values from 3.9‰ – 5.8‰. Field 5a (background site) has the next larger average δ15N ratio of

5.1‰ (0.6 SD) with a range of 3.8‰ – 6.3‰. Field 12 (application site) has the largest average of 5.6‰ (0.7 SD) with a range from 4.2‰ – 6.6‰.

Table 6 – Results for various constituents on each field after 1:1 soil-water extraction method (fluid method).

Constituents	**Field 5a**	**Field 12**	**Field 1**
pH	5.8	6.0	6.7
K (ppm)	6.0	20.7	75.0
Ca (ppm)	38.2	73.5	50.9
Na (ppm)	11.2	12.5	15.2
Mg (ppm)	3.3	6.7	7.4
EC (µS/cm)	488.1	891.9	857.9
TSS (ppm)	322.2	588.6	566.2
PAR (ratio)	0.2	0.4	1.6
SAR (ratio)	0.5	0.4	0.6
EPP (%)	5.0	6.9	16.5
ESP (%)	0.0	0.0	0.0

Table 7 – Results of Total Nitrogen (TN), Total Carbon (TC), and Organic Matter (OM) tests.

Constituents (%)	Field 5a	Field 12	Field 1
Average Total Nitrogen	0.18	0.14	0.09
Average Total Carbon	2.00	1.61	0.92
Average Organic Matter	3.45	2.78	1.58

5.3.3 Statistical Analysis of Soil Data

In Field 5a (background site) for a simple random sample at a 95% confidence interval, a margin of error of 31% was calculated, where *n* is the 10 total samples. Because the number of samples is small, this dataset provides an understanding of the relationship between the variables, but is not statistically strong. The constituents (from both Mehlich-3 and 1:1 soil-water methods) of statistical significance were: pH, Ca, Mg, S, Fe, Cu, Zn, B, and EC. The statistical tests were applied to the two halves of the field divided by soil type. The statistical analysis indicates that they all have a significant difference between the northern and southern parts of the field. This is also apparent in the percentage of sand with the northern portion of the site having a sandier soil.

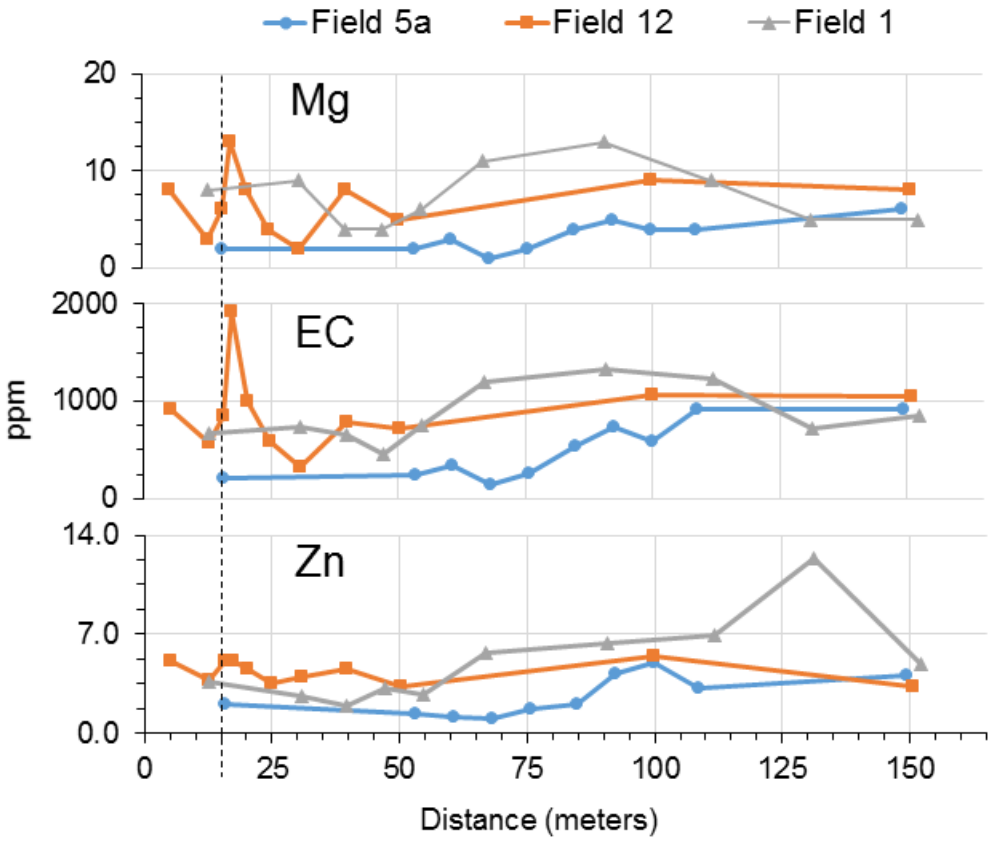

Figure 21 – Soil sampling results plotted showing the constituents of Field 5a were found to be statistically different from the other fields.

In Field 12 (application site) 11 total samples were analyzed. Because the small number of samples, this dataset provides an understanding of the relationship between the variables, but is not statistically strong. The constituents (from both Mehlich-3 and 1:1 soil-water methods) of interest were: pH, P, K, Ca, Mg, S, Cu, Zn, B, fluid EC, and $\delta^{15}N$. The statistical tests were applied to the two groups, the unapplied edge of the field and application zone, of soil samples from the field. The statistical analysis indicates there is not a significant difference between the unapplied edge of the field and application zone. Weak and strong relationship between the constituents and the corresponding resistivity values existed.

In Field 1 (recent application site) 10 total samples were available. The statistical tests could not be applied to the two groups from Field 1 as the unapplied edge of the field and application zone, because there is only one sample in the unapplied edge of the field and that is insufficient for analysis.

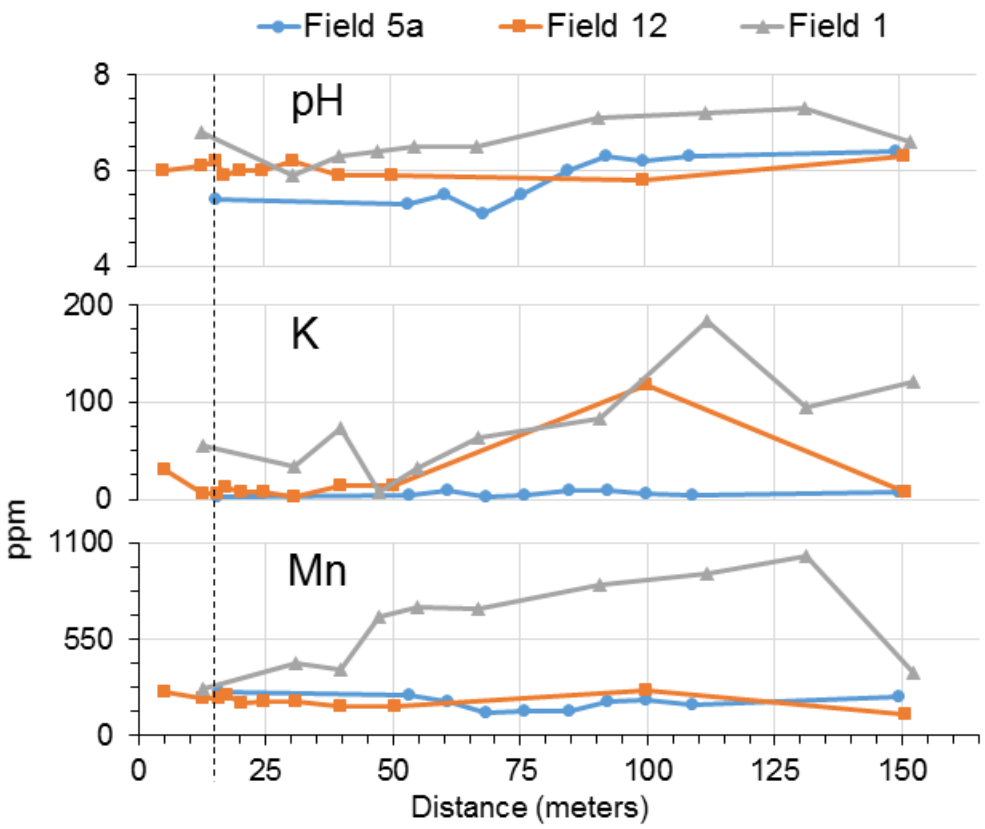

Figure 22 – Soil sampling results plotted showing the constituents of Field 1 were found to be statistically different from the other fields.

To statistically compare the fields against each other, the same t-test was run and compared the constituent of each field. When comparing Field 5a vs Field 1, we find that pH, K, Mg, Mn, Zn, fluid EC, TN, TC, and OM show a significant difference between the two fields. Field 12 vs Field 1, we find that pH, K, Mn, TN, TC, and OM show a significant difference

between the two fields. Field 5a vs Field 12, we find that Ca, Mg, Zn, fluid EC, and TN show a significant difference between the two fields. This results in Field 5a being statistically lower than both Fields 12 and 1 in Mg, Zn, and fluid EC and is statistically higher than both Fields 12 and 1 in TN. Field 1 is statistically higher than both Fields 5a and 12 in pH, K, and Mn and is statistically lower than both Fields 5a and 12 in TN, TC, and OM. Although Field 12 was statistically different in some constituents for one field, it was not statistically different for the other field.

Isotopic signatures were used to find the isotopic signature of swine lagoon effluent. By finding, or not finding, a particular isotopic value indicates whether or not our soil samples contain any trace amounts of swine lagoon effluent. The $\delta^{15}N$ values ranging from 3.8 ‰ – 6.6 ‰ across all three fields. Field 5a has higher average values than Field 1. When comparing this to a compilation of other data we see that this range in values falls on the peaks of "natural" and "fertilized" soils and in fact falls on the far low end for "animal waste" values (Aly et al., 1981; Aravena et al., 1993; Black and Waring, 1977; Bremner and Tabatabai, 1973; Fogg et al., 1998; Freyer, 1978, 1991; Garten, 1992, 1996; Gormly and Spalding, 1979; Heaton, 1986, 1987; Heaton et al., 1997; Hoering, 1957; Kohl et al., 1971; Kreitler, 1975, 1979; Moore, 1977; Paerl and Fogel, 1994; Shearer et al., 1974, 1978; Wolterink et al., 1979). Hog waste $\delta^{15}N$ averages have been recorded to fall within 10 ‰ – 20 ‰ (Fogg et al., 1998; Krietler, 1975, 1979; Wolterink et al., 1979). At this time, the fields do not provide a significant nitrogen isotopic signature in this dataset allowing the separation of signatures for applied manure and background soils.

5.3.4 Site Comparison

Field 5a shows a distinct trend in bulk electrical resistivity data that compares well with soil thickness and soil test results. The electrical resistivity data in Figure 20 shows a much more resistive half of the field is in the north (0-80 m) and a more electrically conductive half of the

field in the south (80-165 m). To the north, the site thins to a rocky soil and to the south it thickens and the soil is composed of finer particles. Figure 21 shows the soil test results for this site and indicate that of the north half of the field has lower values for the three *distinctly different* constituents: Mg, Zn, and fluid EC.

Field 12 appears to have somewhat more electrically conductive soil over a broader area than Field 5a and shows an overall increase in bulk electrical conductivity from 30 m (100 feet). This electrically conductive area is not located near the stream, where application of manure would not occur (unapplied edge of the field) under the recommended protocols of the comprehensive nutrient management plan. The electrical resistivity data shows consistency across the entire field. The soil thickness is also thicker across the entire field when compared to Field 5a. Soil test results showed no indication that Field 12 was statistically different from the other two fields.

Field 1 does not share the same electrical features seen in the alluvium of Fields 5a and 12, but does appear to have more electrically conductive features present within the epikarst zone. The features present show a relatively more resistive soil zone but a *very electrically conductive* epikarst zone that extends nearly the length of the field but dissipates at the unapplied edge of the field, approximately 30 m (100 feet) from the northern edge of the field. This distance from the northern edge of the field is consistent with the recommended protocols of the comprehensive nutrient management plan for where the application of manure would not occur. The soil here on this site was thin and rocky and grain size analysis showed that this site was different than the other two sites. Figure 22 shows the soil test results for this site and indicate three *distinctly different* constituents are higher than the other two sites.

The anticipated ERI relationship with fluid EC of soil water samples would be that as electrical conductivity of the fluid increased, the bulk resistivity of the soil would decrease. There was no strong relationship between these parameters for the lower resolution (1.5 m) datasets.

While these datasets showed that the applied fields had a higher bulk conductivity (lower resistivity) than the background sites, the datasets averaged too deeply into the subsurface leading to some significant contrasts at the surface between the two ERI dataset resolutions.

For the higher resolution dataset, the expected the relationship held for the background site, Field 5a (Figure 23). The fluid EC has an inverse relationship with bulk resistivity with an r^2 value of 0.56. For the applied fields, the fields have a positive relationship with higher EC fluids resulting in higher resistivity zones with an r^2 value of 0.50 for Field 12 and 0.98 for Field 1. This type of relationship indicates that the bulk electrical properties are not only responding to the addition of a fluid with a higher electrical conductivity, but that another soil electrical property must be changing as well. Pettyjohn et al. (1986) may have stated the obvious, but it's worth noting here, "whatever the final conclusions are, it is evident that one should expect the unexpected."

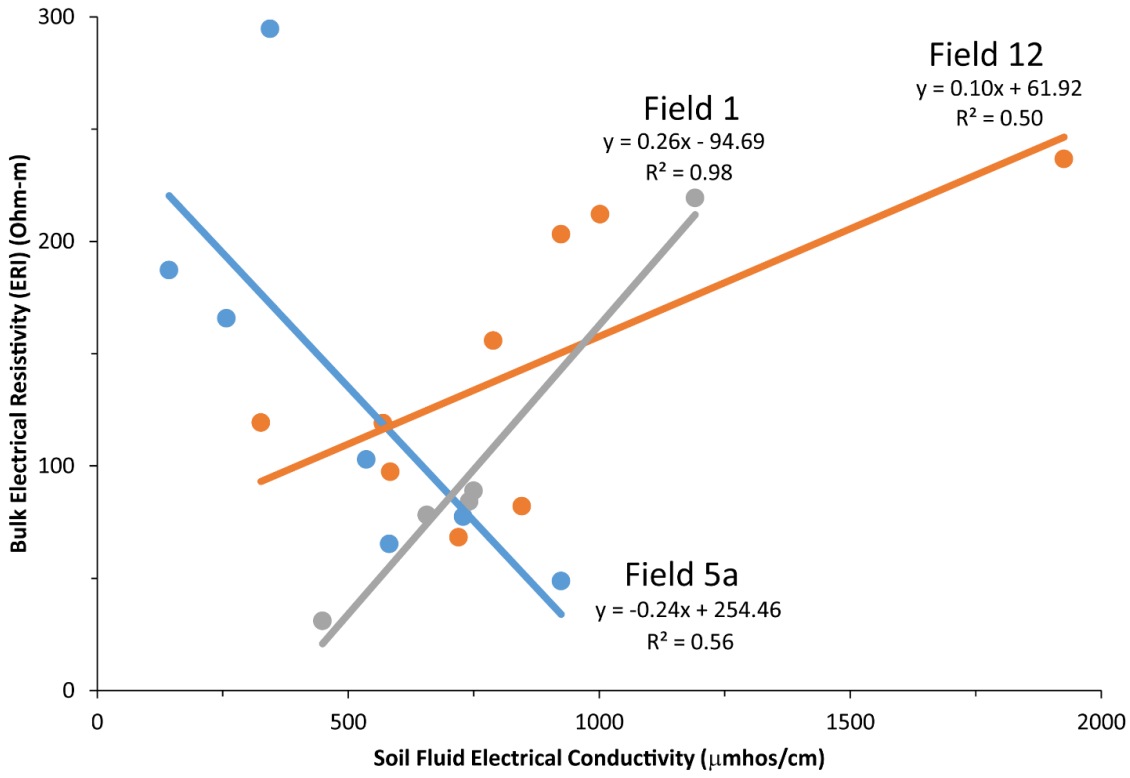

Figure 23 – Soil Fluid Electrical Conductivity measured from soil samples collected along three ERI transects compared with ERI bulk resistivity data with 0.5 meter resolution for three fields near Mount Judea, Arkansas. Field 5a is the background site and Fields 1 and 12 had applied swine lagoon effluent.

5.4 Numerical Modeling

To determine the movement of swine lagoon effluent in the subsurface, numerical modeling was conducted on a simulated soil column. After simulating a swine lagoon effluent application and 13 rainfall events, sequentially followed by 13, 27-day breaks of no rain, we see movement of Ca, K, S, through the system and sorption of Mg, Fe, Mn, Zn, and Cu near the surface (Figure 30). After each rainfall event, concentrations of each constituent dropped slightly and those more mobile constituents moved closer and closer to the simulated water table. The differences in K_D values are demonstrated in the concentration profiles of the more mobile (lower

K_D values) ions (Figure 24 and Figure 25) and the less mobile (higher K_D values) ions (Figure 26 and Figure 27). The figures depicting initial conditions show sharp increases in concentration of these constituents near the top of the soil column but these are artifacts of where initial conditions were set.

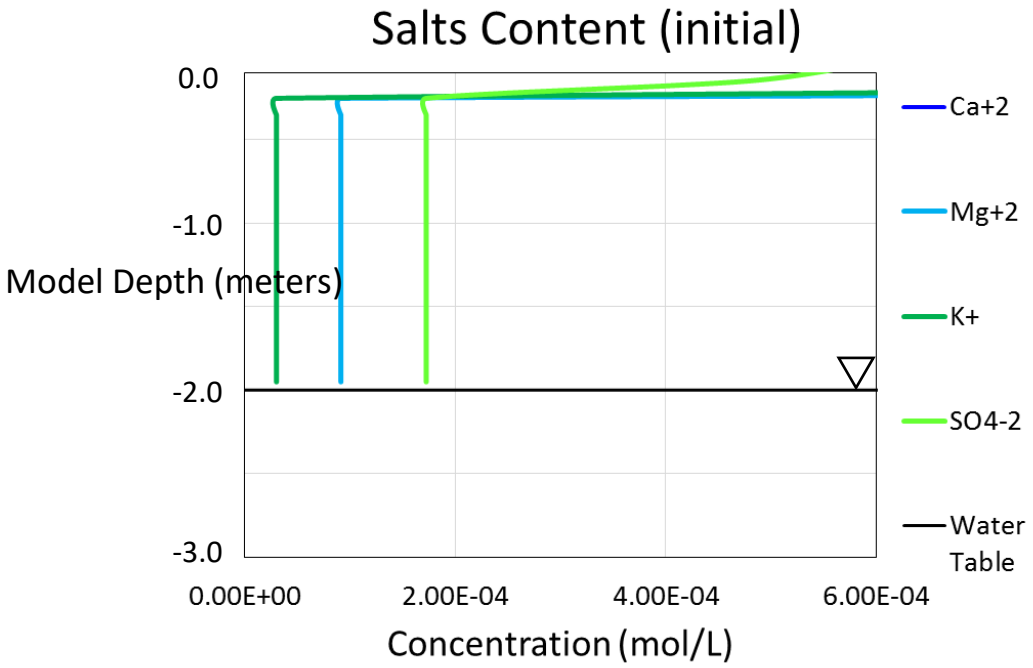

Figure 24 – Initial concentration profile of more mobile (lower K_D value) ions.

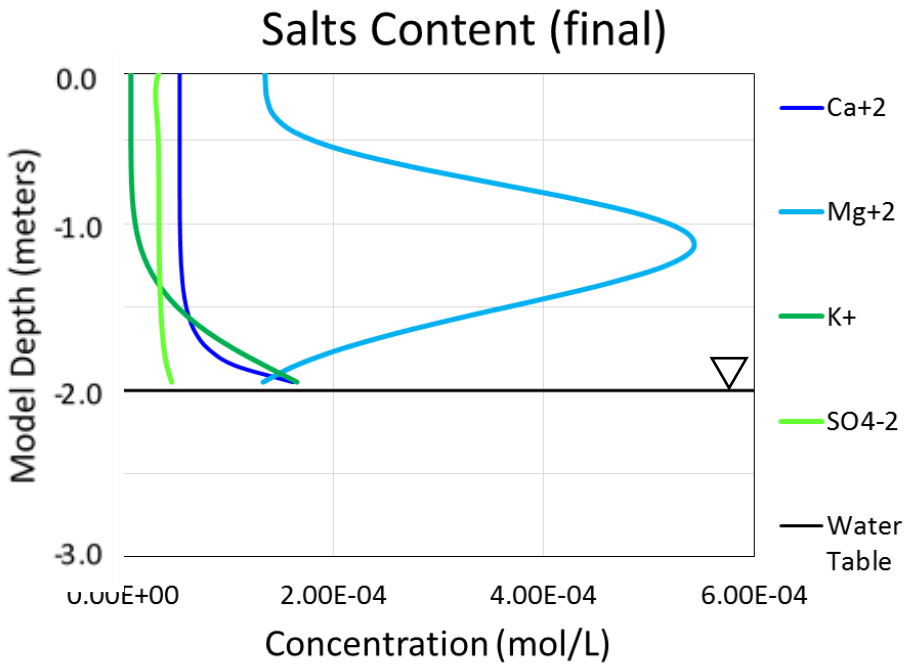

Figure 25 – Final concentration profile of more mobile (lower K_D value) ions.

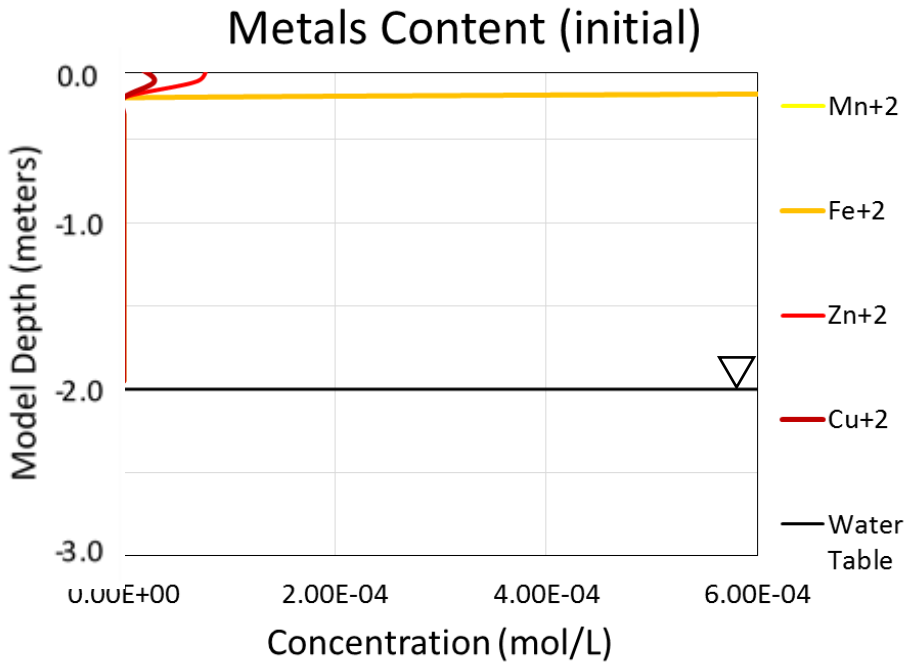

Figure 26 – Initial concentration profile of less mobile (higher K_D value) ions.

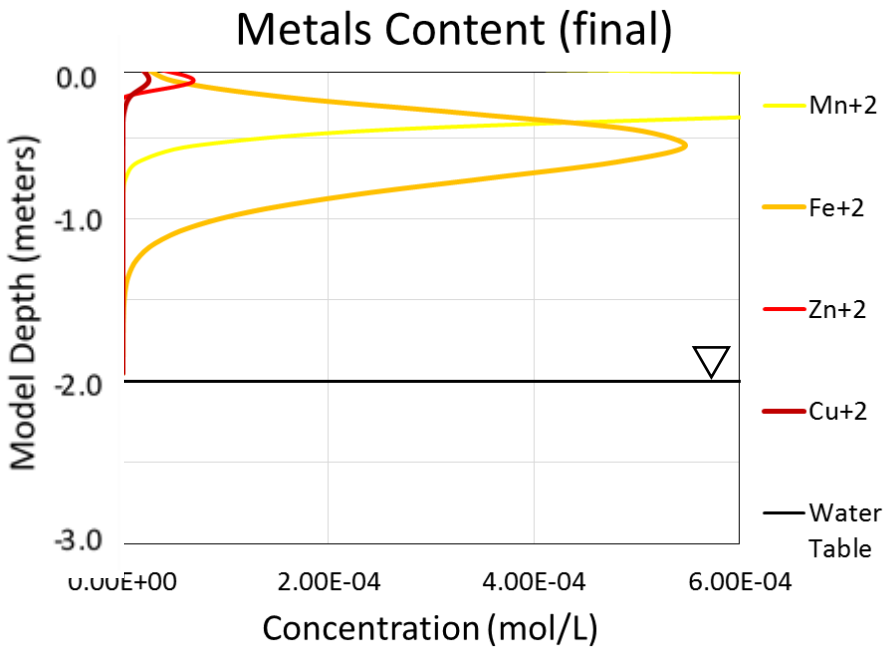

Figure 27 – Final concentration profile of less mobile (higher K_D value) ions.

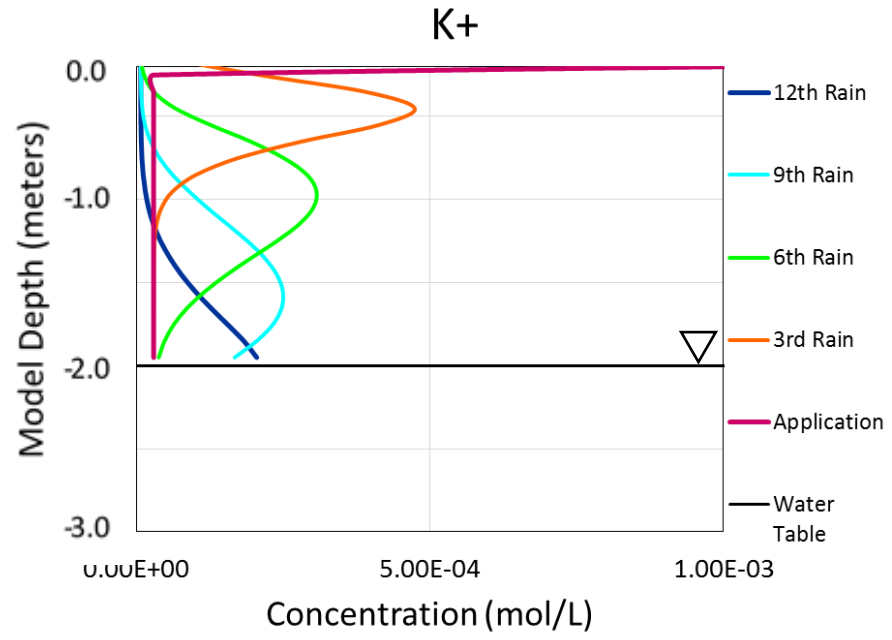

Figure 28 – K concentration profile after effluent application, and the 3rd, 6th, 9th, and 12th rain events.

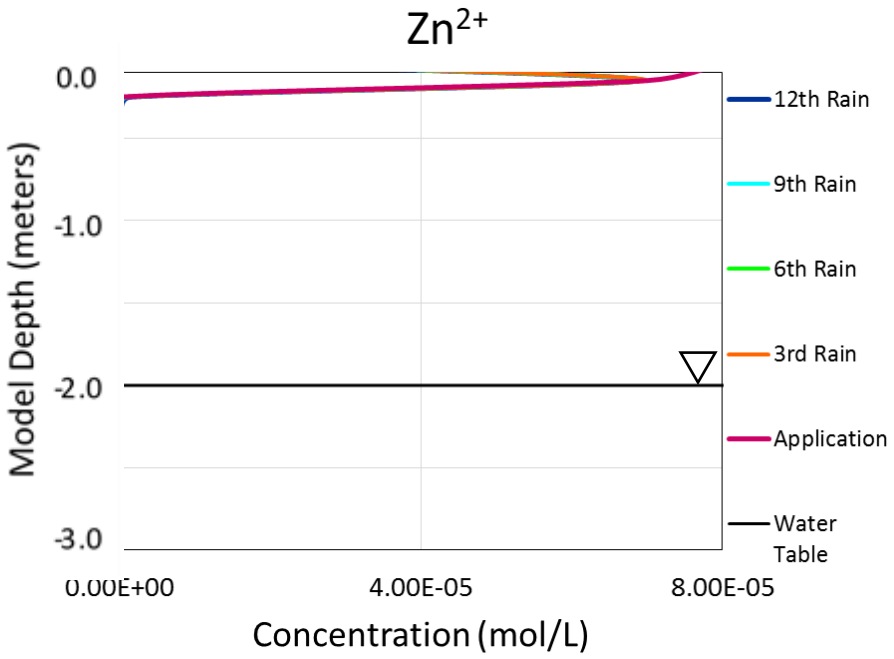

Figure 29 – Zn concentration profile after effluent application, and the 3rd, 6th, 9th, and 12th rain events.

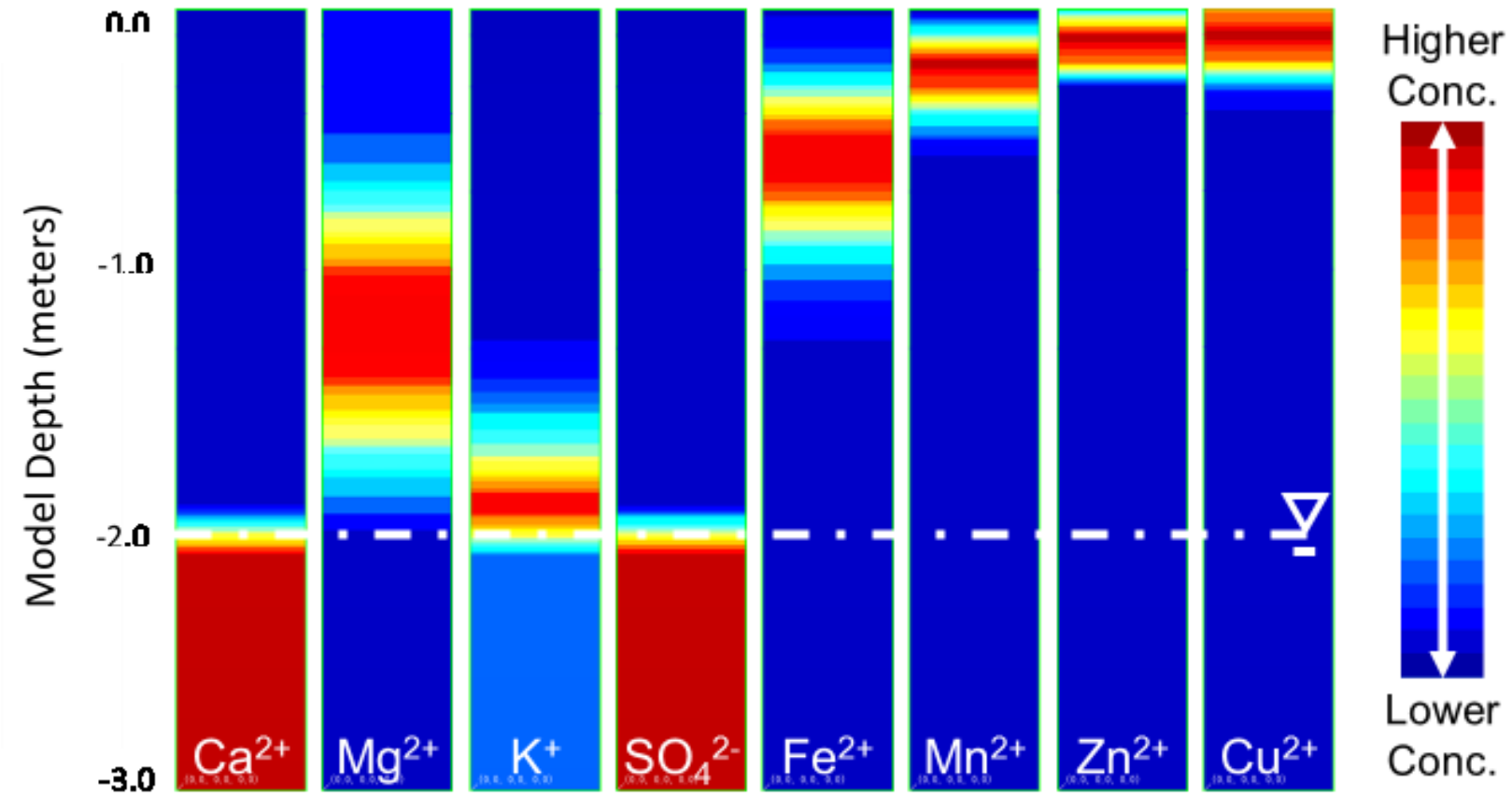

Figure 30 – TOUGHREACT simulation results: 365 simulated days after swine lagoon effluent. In the image, red represents higher concentrations and blue represents lower concentrations.

CHAPTER 6

6.0 DISCUSSION

Collecting pseudo 3D bulk electrical resistivity data allowed for field-scale datasets that estimate local variability in geology. After the field-scale correlations were determined (inverse relationship between bulk resistivity and soil fluid EC) for the background field, we attempted to find correlations on the local-scale to explain the opposing trend (positive relationship between bulk resistivity and fluid EC) on the applied fields (Figure 23). In this section, we evaluate and discuss three possible questions for why the applied sites are more electrically conductive than the background site: 1) are the applied fields more electrically conductive due to higher EC fluids applied to the fields (bulk electrical resistivity and the relationship with fluid EC), 2) are the applied fields more conductive due to biological activity (organic content of each site for effects of microbes), and 3) are the applied fields more conductive due to metal deposition (metal signatures of the swine lagoon effluent)?. Fields 5a and 12 share some electrical and geologic characteristics but there are a few distinctions that are important. Field 1 on the other hand is different from the other two sites in many aspects. Soil analysis is a complex issue that makes possible correlations between constituent levels a difficult task and much of the literature finds that individual site testing is required to better understand specific properties of a given site.

6.1 Bulk Electrical Resistivity and Fluid Electrical Conductivity

The electrical structure of the soil, epikarst, and bedrock were consistent with the literature of weathered mantled carbonate bedrock areas (Benson, 1995; Carriere et al., 2013;

Gambetta et al., 2009; Halihan et al., 2005, 2009; Miller et al., 2014; Pellicer and Gibson, 2011; Schwartz and Schreiber, 2009; Stepisnik and Mihevc, 2008). The soil thickness increasing towards the streams would be expected in an alluvial valley. The epikarst zone having significant variability in lateral and vertical properties was consistent with evaluations from other carbonate locations (Gambetta et al., 2009; Halihan et al., 2005, 2009; Pellicer and Gibson, 2011). The data are consistent with previous investigations (Bolyard, 2007; Halihan et al., 2005, 2009) that indicate that more permeable flowpaths would exist in the bedrock of the site, but no drilling or hydraulic testing data are available from the sites included in this investigation.

It is known that resistivity and conductivity are inverse of each other. When evaluating a site using geophysics, typical trends of the site follow that as the electrical conductivity of the subsurface fluid increases, the bulk resistivity of the entire subsurface (fluid, soil, rock, air, etc.) decreases. The data from the two applied sites indicated the opposite is the case for these fields (Figure 23). The more electrically conductive a single soil fluid sample was on either field, at that same location, the bulk resistivity of the ERI was higher than the other samples. We evaluated the datasets to determine if data from a nearby resistivity model cell was influencing this behavior or if the model resistivity value itself was abnormal data, but we did not find a point where either dataset had significant variability near our samples. We then evaluated the most electrically conductive soil samples (measured using 1:1 soil to water extraction method) to see if they were also the most electrically resistive of the ERI. That was not the case either. Those high points also included some of the less resistive, bulk resistivity values, but still ended up following the overall trend with acceptable r^2 values (detailed in section 5.3.4) (Figure 23). The soil fluid EC on the applied fields do not appear to control the conductance observed in bulk ER datasets and it is unknown whether inorganic nitrogen is a control of fluid EC in this case as seen in other studies (Racz and Fitzgerald, 2000). Correlations were found between the bulk datasets of bulk resistivity

and fluid EC and between fluid EC and Zn and a correlation on a point-by-point basis could not be determined.

Heavy precipitation before and during trips in December 2014 and March 2015 may have affected soil sampling. Runoff can mobilize land applied constituents, when rainfall closely follows application (Iqbal and Krothe, 1995; Sharpley, 1985; Smith et al., 2007). An increase in total number or depth of soil samples could strengthen statistical correlations as well as possibly refine them to a point-by-point scale; however, sampling deeper would require a rock coring method. Further monitoring of the epikarst, karst, and bedrock may be required as chemical compounds generated from the addition of swine lagoon effluent applications could increase the weathering effects on the bedrock below. This was not part of the study but is worth noting for future studies.

6.2 Soil Chemistry by Site

The results of the chemical and physical analysis of the soil is representative of the conditions on each field, but are small datasets for the fields overall relative to literature evaluations of soil chemistry on the field scale (Choudhary et. al, 1996; DeRouchey et. al, 1999; Hannan, 2011; Klimek, 2012; Plaza et. al, 2004; Smith et. al, 2007; Suhadolc et. al, 2004; Turner et. al, 2010). The primary use of the soil sampling was to evaluate parameters that may change with electrical properties and provide future indicator parameters for geophysical soil monitoring. Some constituents were found to be statistically significant on particular fields and when compared to previous studies, were pertinent to this study (Choudhary et. al, 1996; DeRouchey et. al, 1999; Hannan, 2011; Klimek, 2012; Plaza et. al, 2004; Smith et. al, 2007; Suhadolc et. al, 2004; Turner et. al, 2010). However, the levels of constituents for Fields 12 and 1 were not sufficient to definitively indicate the presence of swine lagoon effluent when compared to literature values. Although, the data do show that Fields 12 and 1 have consistently higher values

for many of the constituents than Field 5a, but plant uptake and removal would govern application amounts for swine lagoon effluent as to prevent any excess buildup of particular constituents (Racz and Fitzgerald, 2000).

Field 5a was statistically lower in Mg, Zn, and fluid EC, but higher in TN than the other two fields. Studies show Mg levels in soils can be higher due to natural causes from the weathering of limestone (Hannan, 2011; Plaza et. al, 2004) or anthropogenic causes due to applied swine lagoon effluent (Schoenau, 2006). Field 5a sits primarily on alluvium and does not receive swine lagoon effluent, but is statistically lower than Field 12 which is in the same geologic setting. Lower levels of zinc on the background site are consistent with previously published values, as swine lagoon effluent can carry increased levels of zinc (Klimek, 2012; Lukman et al., 1994; Murdock and Lowe, 2001; Racz and Fitzgerald, 2000; Suhadolc et. al, 2004). Lower fluid EC on the background site is consistent with the swine lagoon effluent soil amendments having higher fluid EC (Turner et. al, 2010) but can also be found in cases were nutrient content or inorganic nitrogen are low (Racz and Fitzgerald, 2000). The fluid EC relationship on a point-by-point basis with other constituents requires further study.

Field 1 was statistically higher in pH, K, and Mn, but lower in TN, TC, and OM than the other two fields. Levels of K can be altered by the type of feed given to swine on fields receiving manure (Racz and Fitzgerald, 2000; Schoenau, 2006) and result from materials weathering from carbonates (Hannan, 2011). Some fields, where the soil is developed from a limestone layer beneath it, can have higher pH levels compared to the background site with alluvium soil (Plaza et. al, 2004). Scientific literature on the relation of manganese with applied swine lagoon effluent was not found.

6.3 Organics Content

Microbes, in large enough communities, can be detected by ERI as increased electrical conductivity due to the conversion of OM to energy, alteration to fluid chemistry or size of the pores, or from the biomass of microbes (Atekwana and Atekwana, 2010). If microbial populations are developing to consume the available applied material, this type of relationship between the bulk and fluid properties may occur. Previous soil studies have examined applied nitrate and ammonium and found signatures of swine lagoon effluent on sites, however, we did not examine these two constituents in our sampling. Clay mineral structure has been found to correlate with the sorption of metals (REF) but this data was not available. Additional research on the microbial populations, nitrate and ammonium, or clay structure would be required to evaluate these factors. As proxies for microbial activity, we evaluated TC, TN, and OM contents (Atekwana and Atekwana, 2010) in soil samples up to a depth of 10 cm (4 inches). The highest OM content should reside in the topsoil and be upwards of 5% for fertile soils (Mitchell and Everest, 1995). It is known though, that constituent levels tend to increase over time as fertilizers are applied (Carpenter et al., 1998; Choudhary et. al, 1996; Hannan, 2011; Reddy et al., 1980; Schoenau, 2006) and it "may take several years of application before significant differences can be detected" (Schoenau, 2006). We see that not only is the OM content on the two applied sites lower than the background site, but we also see that the most recently applied site has the lowest OM content of the three sites (Table 7). If OM were low due to microbial consumption, this could support both the lowest OM levels as well as the lowest electrically resistivity being on the most recently applied to site. This would mean the signatures on Field 12 come from inactive microbes (a biomass or biofilm) and hence the higher, yet not highest, OM content. However, for microbial activity to be causing higher electrical conductivity on the applied sites, the community would need to be large enough for detection and would require OM on the applied sites to be higher than the background, as well as correlating chemical signatures from the soil water (Atekwana and

Atekwana, 2010; Frankenberger and Dick, 1983). We also see that if there is typically low nutrient content and OM, low fluid EC is associated (Racz and Fitzgerald, 2000). As applied effluent is not expected to provide a strong fertilizing effect to the soil immediately, a lack of microbial signatures is not unexpected based on previous literature (Atekwana and Atekwana, 2010; Carpenter et al., 1998; Choudhary et. al, 1996; Frankenberger and Dick, 1983; Hannan, 2011; Racz and Fitzgerald, 2000; Reddy et al., 1980; Schoenau, 2006; Sharpley, 1985).

6.4 Metals Content

Of the measured chemical constituents that were statistically significantly different between fields (Figure 21 and Figure 22), Zn was the only one found that correlates well with fluid EC for all sites, with R^2 of 0.50, 0.38, and 0.60 for Field 5a, Field 12, and Field 1, respectively. For metals to influence fluid EC, there must be metals in solution. Zn will begin to drop out of solution at pH's as low as 5.6, but have been reported to average from 6.0-7.0 (Luxton et al., 2013; Perelomov et al., 2011; Racz and Fitzgerald, 2000; Schulte, 2004). Metals are found to precipitate more in cases with increased OM or $CaCO_3$ (lime) (Akay and Doulati, 2012; Lukman et al., 1994; Luxton et al., 2013), however, we can only see this as possible for Field 1 due to its locally derived soil (since both applied sites are lower in OM). Metals such as Zn will coexist in solution and as precipitates depending on pH fluxes. If enough of the metals stay in solution, fluid EC could increase with metal content and if soil grains become coated with Zn (or any metal) plating, this could be a cause for why we see the two applied sites as more electrically conductive on a bulk electrical resistivity basis. Although Zn is the only metal to correlate well with fluid EC, it is most plausible to say it is a combination of the metals from the swine effluent that increases both fluid EC and overall electrical conductance on the field scale. This still does not provide a simple explanation of the positive relationship between fluid EC and bulk resistivity.

6.5 Reactive Transport

The results of modeling a swine lagoon effluent application to a soil column behaved as expected. Limiting factors included K_D values for each constituent and simulated rainfall amounts. Advection processes were demonstrated (Figure 28) during the rain events which allow those ions with smaller K_D values the ability to move while other ions sorb to the soil near the surface. The annual rainfall for the site was included in just 13 (1-year, 24-hour events) simulated rainfall events to attempt to capture larger storm events. If smaller events were used, it should delay some migration, but that the same overall pattern would be expected to occur with a longer timescale to reach it. Although these were scenarios developed in the model, we found that upon each trip to the field sites, the ground was saturated from rains the prior day which could have diluted soil samples by infiltration. It is possible that signatures in the ER images may not be detectable in soil samples because of this dilution (Iqbal and Krothe, 1995; Sharpley, 1985; Smith et al., 2007). However, in order for this to be true, both electrically conductive sites would had to have received applications near the same relative time rather than months apart. ER data collected on Field 12 during both trips saw similar signatures on each set of images, indicating no significant changes to the site between sampling events. Deep soil samples are not available to test the hypotheses at depth. Deeper samples would provide information on the distribution of materials throughout the soil column, assist in understanding of the subsurface reactions, and calibrate the model. In the shallow soil samples that were collected, regardless of soil sample dilution, X-Ray Diffraction could be useful to determine clay mineral structure which would improve sorption parameters of the model. The 2:1 and 2:1:1 clay mineral structures have been found to be quality sorption sites for metals (Akay and Doulati, 2012). However, this test was not conducted in this study. This could further support the hypothesis that metal precipitation on soil grains as the most plausible explanation for the observed signatures at the sites. Generating multiple models with different environments, similar to other fields receiving swine lagoon

effluent applications, would be useful for understanding the possible influence of flowpaths on effluent transport.

CHAPTER 7

7.0 CONCLUSIONS

A field experiment was conducted to determine the hydrogeophysical properties of applied swine effluent to determine if signatures were available to monitor fluid transport through a mantled karst. The field data collected in Mount Judea, Arkansas, in December 2014 and March 2015 characterizes the subsurface of a background site (Field 5a) and two swine effluent application sites (Fields 12 and 1) using ERI, soil analysis, and numerical modeling. The electrical structure of the sites included the determination of three separate lithologic zones (bedrock, epikarst, and soil) and opposing electrical trends between unapplied and applied effluent sites. Soil analysis provided chemical characterization of each site. A numerical model was created to analyze subsurface flow of simulated swine effluent. These results were useful in defining the characteristics of the soil zone, epikarst zone, and the bedrock and anticipated subsurface chemical transport. The take-away is that over time, constituents will build up in the soil and it is expected that by evaluating the metals and OM content one could determine swine lagoon effluent relative concentrations across the fields. Using ERI allows for a quick characterization of the bulk electrical signatures generated by metals concentrations and the possible microbial activity, given required increases in OM content across the sites.

7.1 Electrical Structure

ERI surveys contributed to understanding the structure and distribution of material underlying Fields 5a, 12, and 1. The surveys confirmed the soil thickness, presence, extent, and

depth of epikarst features and bedrock material and highlights possible dissolution features and fracturing typical of this geologic formation. The average soil thickness across the sites is very similar (1-4.5 m or 3-14.75 feet), except for the area in which Field 5a exhibits thinning of the soil (to 0.5 m or 1.5 feet). Field 1 had a soil thickness of 0.5 m (1.5 feet). The epikarst thickness is similar on both Fields 5a and 12 with a range of 2-23 m thick (6.5-75 feet), with an average of approximately 7 m (23 feet), but the distribution of possible fracturing in bedrock or karst features was variable as expected. There was not confirmation drilling at the sites to evaluate the rock properties of the epikarst zone, but the results are consistent with other investigations of epikarst zones (Pellicer and Gibson, 2011; Williams, 2008).

The ERI surveys showed the applied sites were more electrically conductive than the background sites. When comparing the ERI and soil sampling bulk datasets, the results show strong trends between bulk resistivity and fluid EC. The trend on the background site behaves as expected (inverse relationship), but the trend for the applied sites is an opposing trend and unexpected (positive relationship).

7.2 Soil Analysis

Soil sampling showed that there are statistically significant chemical differences between the sites. The background site (Field 5a) had consistently lower concentrations of many of the measured soil parameters but is only statistically lower in Mg, Zn, and soil fluid EC, while it was highest in OM content. Field 5a is only statistically higher (than the other fields) in TN though. Field 12 is only statistically different from either site in TN, although being higher than Field 5a in many soil properties, except the organic components. Field 1 has consistently higher values in many of the soil parameters, but was only statistically higher (than the other fields) in pH, K, and Mn and while it was lowest in the organics, it is statistically different in TC, TN, and OM. These results show that statistical differences can be observed in certain constituents for recently applied

areas on a field-by-field scale but were not determined on a point-by-point scale. With lower amounts of application or over time, these signatures may not be detectable.

To explain the unexpected trend in ERI vs fluid EC for the applied sites, soil analysis allowed for other correlations. Zn correlated with fluid EC for all sites but not with bulk ER. Zn and other metal ions sorbing to soil grains are the most plausible for explaining increases in fluid EC and the site-to-site difference in bulk conductance. Total N, TC, and OM trended in the opposite direction than what was expected, with the most recently applied site containing the lowest concentrations. Because OM was low on the applied sites and previous literature indicating that impacts from effluent fertilizers take multiple applications before being noticed, microbial activity is not considered a cause for the unexpected trend (ERI vs fluid EC) on the applied sites.

7.3 Numerical Modeling

Numerical modeling demonstrated the possible subsurface reactions of the highlighted constituents; the more mobile ions moved through the system while the less mobile ions sorbed to the soil grains nearer the surface. The sorption parameters are controlled by K_D values input into the model, so site-specific determination of those values would provide better resolution of expected depths of concentration of the constituents. Deeper soil sampling and X-Ray Diffraction would be useful going forward to better characterize the soil transport properties and constrain the model. The model results illustrate possible outcomes if the concentrations of applied swine effluent are increased or decreased. The model would best be used to examine those changes over time and predict reactions in the soil column utilizing Zn as a proxy for determining the loadings and responses.

8.0 REFERENCES

Adeli, A., Bolster, C.H., Rowe, D.E., McLaughlin, M.R., and Brink, G.E., 2008, Effect of long-term swine effluent application on selected soil properties *in* Soil Science, 173(3), 223-235 p.

Adeli, A., Varco, J.J., Mostafa, S.M., Rowe, D.E., and Bala, M.F., 2002, Comparability of anaerobic swine lagoon effluent to commercial fertilizer on soil nutrient dynamics *in* Communications in Soil Science and Plant Analysis, 33(19-20), 3779-3795 p.

Akay, A. and Doulati, B., 2012, The effect of soil properties on Zn adsorption *in* Journal of International Environmental Application & Science, 7(1), 151-160 p.

Allaby, M., eds., 2008, A dictionary of earth sciences: Oxford University Press, Oxford Reference.

Allred, B.J., Ehsani, M.R., and Daniels, J.J., 2003, The impact on electrical conductivity measurements due to soil profile properties, shallow hydrologic conditions, fertilizer application, agricultural tillage, and the type of geophysical method employed *in* paper presented at the 16th EGGS Symposium on the Application of Geophysics to Engineering and Environmental Problems, San Antonio, TX, 336–349 p.

Aly, A.I.M., Mohamed, M.A., and Hallaba, E., 1981, Mass spectrometric determination of the nitrogen-15 content of different Egyptian fertilizers *in* Journal of Radioanalytical Chemistry, 67(1), 55-60 p.

Anderson, D., 2012, Organic matter in prairie soils *in* Crops & Soils, 4-10 p.

Anderson, M.S., 1960, History and developments of soil testing *in* Agricultural and Food Chemistry, 8(2), 84-87 p.

Aravena, R., Evans, M.L., and Cherry, J.A., 1993, Stable isotopes of oxygen and nitrogen in source identification on nitrate from septic systems *in* Ground Water, 31(2), 180-186 p.

Atekwana, E.A., and Atekwana, E.A., 2010, Geophysical signatures of microbial activity at hydrocarbon contaminated sites: a review *in* Surveys in Geophysics, 31, 247-283 p.

Benson, A.K., 1995, Applications of ground penetrating radar in assessing some geological hazards: examples of groundwater contamination, faults, cavities *in* Journal of Applied Geophysics, 33, 177-193 p.

Berkowitz, B., 2002, Characterizing flow and transport in fractured geological media: a review *in* Advances in Water Resources, 25, 861-884 p.

Big Creek Research and Extension Team, 2013, Demonstrating and monitoring the sustainable management of nutrients on C&H Farm in Big Creek Watershed: quarterly report – October 2013 to December 2013, 96 p.

Black, A.S. and Waring, S.A., 1977, The natural abundance of 15N in the soil-water system of a small catchment area *in* Australian Journal of Soil Research, 15, 51-57 p.

Bolyard, S.E., 2007, Migration of landfill contaminants in a tilted-block mantled-karst setting in northwestern Arkansas, University of Arkansas, M.Sc. thesis, 69 p.

Brady, N.C. and Weil, R.R., 2002, The Nature and Properties of Soils 13th Edition: Upper Saddle River, NJ: Prentice Hall, Print.

Bremner, J.M. and Tabatabai, M.A., 1973, Nitrogen-15 enrichment of soils and soil-derived nitrate *in* Journal of Environmental Quality, 2(3), 363-365 p.

Broetto, T., Tornquist, C.G., Bayer, C., Campos, B.C., Merten, C.G., and Wottrich, B., 2014, Soils and surface waters as affected by long-term swine slurry application in oxisols of Southern Brazil *in* Pedosphere, 24(5), 585-594 p.

Brunet, P., Clément, R., and Bouvier, C., 2010, Monitoring soil water content and deficit using electrical resistivity tomography (ERT) – a case study in Cevennes area, France *in* Journal of Hydrology, 380, 146-153 p.

Carrière, S.D., Chalikakis, K., Sénéchal, G., Danquigny, C., and Emblanch, C., 2013, Combining electrical resistivity tomography and ground penetrating radar to study geological structuring of karst unsaturated zone *in* Journal of Applied Geophysics, 94, 31-41 p.

Carpenter, S.R., Caraco, N.F., Correll, D.L., Howarth, R.W., Sharpley, A.N., and Smith, V.H., 1998, Nonpoint pollution of surface waters with phosphorus and nitrogen *in* Ecological Applications, 8(3), 559-568 p.

Celia, M.A., Kindred, J.S., and Herrera, I., 1989, Contaminant transport and biodegradation: a numerical model for reactive transport in porous media *in* Water Resources Research, 25(6), 1141-1148 p.

Chamberlain, A.T., Sellers, W., Proctor, C., and Coard, R., 2000, Cave detection in limestone using ground penetrating radar *in* Journal of Archaeological Science, 27, 957-964 p.

Chandler, A.K. and Ausbrooks, S.M., revised 2015, Geologic map of the Mt. Judea quadrangle, Newton County, Arkansas: Arkansas Geologic Survey Digital Map, DGM-AR-00590, 1:24,000.

Chen, D.J.Z. and MacQuarrie, K.T.B., 2004, Numerical simulation of organic carbon, nitrate, and nitrogen isotope behavior during denitrification in a riparian zone *in* Journal of Hydrology, 293, 235-254 p.

Choudhary, M., Bailey, L.D., and Grant, C.A., 1996, Review of the use of swine manure in crop production: effects on yield and composting and on soil and water quality *in* Waste Management & Research, 14, 581-595 p.

Comegna, V., Coppola, A., and Comegna, A., 2011, Laboratory-scale study on reactive contaminant transport in soil by means of one-dimensional advective dispersive models *in* Journal of Agricultural Engineering, 3, 1-6 p.

Corwin, D.L. and Lesch, S.M., 2005, Apparent soil electrical conductivity measurements in agriculture *in* Computers and Electronics in Agriculture, 46, 11-43 p.

Corwin, D.L. and Lesch, S.M., 2003, Application of soil electrical conductivity to precision agriculture: theory, principles, and guidelines *in* Agronomy Journal, 95(3), 455-471 p.

Dane, J.H. and Topp, G.C. (eds), 2002, Methods of soil analysis: Part 4 physical methods, Madison, WI: Soil Science Society of America, Inc., Print.

Davis, R. and Zhang, H., 2001, Plant nutrients in rainfall, PT 2001-21, 1 p.

DeGroot, P.A., 2004, Handbook of stable isotope analytical techniques Volume 1, Amsterdam: Elsevier, Print.

Deng, S.P., Moore, J.M., and Tabatabai, M.A., 2000, Characterization of active nitrogen pools in soils under different cropping systems *in* Biology and Fertility of Soils, 32, 302-309 p.

Deng, S.P., Parham, J.A., Hattey, J.A., and Babu, H.D., 2006, Animal manure and anhydrous ammonia amendment alter microbial carbon use efficiency, microbial biomass, and activities of dehydrogenase and amidohydrolases in semiarid agroecosystems *in* Applied Soil Ecology, 33, 258-268 p.

DeRouchey, J.D., Keeler, G.L., Goodband, R.D., Nelssen, J.L., Tokach, M.D., and Dritz, S.S., 1999, Manure composition from Kansas swine lagoons *from* Swine Day 1999, 3 p.

Espinoza, L., Slaton, N., and Mozaffari, M., 2016, Understanding the numbers on your soil test report, FSA2118, 4 p.

Field, M.S., 2002, A lexicon of cave and karst terminology with special reference to environmental karst hydrology: Washington, D.C., United States Environmental Protection Agency, 214 p.

Ferguson, J.G., 1920, Outlines of the geology, soils and minerals of the state of Arkansas: Little Rock, State Bureau of Mines, Manufactures and Agriculture, 182 p.

Fogg, G.E., Rolston, D.E., Decker, D.L., Louie, D.T., and Grismer, M.E., 1998, Spatial variation in nitrogen isotope values beneath nitrate contamination sources *in* Ground Water, 36(3), 418-426 p.

Fowlkes, D.H., McCright, R.T., and Lowrance, J.S., 1988, Soil Survey of Newton County, Arkansas: Soil Survey, U.S. Department of Agriculture, Soil Conservation Service, 188 p.

Fraisse, C.W., Sudduth, K.A., and Kitchen, N.R., 2001, Delineation of site-specific management zones by unsupervised classification of topographic attributes and soil electrical conductivity *in* American Society of Agricultural Engineers, 44(1), 155-166 p.

Frankenberger, W.T., Jr. and Dick, W.A., 1983, Relationships between enzyme activities and microbial growth and activity indices in soil *in* Soil Science Society of America Journal, 47, 945-951 p.

Freyer, H.D., 1978, Seasonal trends of NH4+ and NO3- nitrogen isotope composition in rain collected at Julich, Germany *in* Tellus, 30, 83-92 p.

Freyer, H.D., 1991, Seasonal variation of 15N/14N ratios in atmospheric nitrate species *in* Tellus, 43B, 30-44 p.

Galloway, J.M., 2004, Hydrogeologic characteristics of four public drinking-water supply springs in northern Arkansas: U.S. Geological Survey Water-Supply Paper 03-4307, 68 p.

Gambetta, M., Armadillo, E., Carmisciano, C., Stefanelli, P., Cocchi, L., and Tontini, F.C., 2011, Determining geophysical properties of a near-surface cave through integrated microgravity vertical gradient and electrical resistivity tomography measurements *in* Journal of Cave and Karst Studies, 73(1), 11-15 p.

Garten, C.T., Jr., 1992, Nitrogen isotope composition of ammonium and nitrate in bulk precipitation and forest throughfall *in* International Journal of Environmental Analytical Chemistry, 47, 33-45 p.

Garten, C.T., Jr., 1996, Stable nitrogen isotope ratios in wet and dry nitrate depostion collected with an artficial tree *in* Tellus, 48B, 60-64 p.

Gary, M.O., Halihan, T., and Sharp, J.M. Jr., 2009, Detection of sub-travertine lakes using electrical resistivity imaging, Sistema Zacatón, Mexico *in* paper presented at the 15th International Congress of Speleology, Kerrville, TX., 2009, Proceedings: Kerrville, TX., International Congress of Speleology, Volume 1, 618 p.

Giao, P.H., Chung, S.G., Kim, D.Y., and Tanaka, H., 2003, Electric imaging and laboratory resistivity testing for geotechnical investigation of Pusan clay deposits *in* Journal of Applied Geophysics, 52, 157-175 p.

Gilley, A.D., 1995, Ammonia volatilization during land application of swine lagoon effluent, Iowa State University, M.Sc. thesis, 95 p.

Gollehon, N. Caswell, M., Ribaudo, M., Kellogg, R., Lander, C., and Letson, D., 2001, Confined animal production and manure nutrients, Agricultural Information Bulletin No. 771, 39 p.

Gormly, J.R. and Spalding, R.F., 1979, Sources and concentrations of nitrate-nitrogen in ground water of the Central Platte Region, Nebraska *in* Ground Water, 17(3), 291-301 p.

Gu, C. and Riley, W.J., 2010, Combined effects of short term rainfall patterns and soil texture on soil nitrogen cycling – a modeling analysis *in* Journal of Contaminant Hydrology, 112, 141-154 p.

Halihan, T., Love, A., and Sharp, J.M., Jr., 2005, Identifying connections in a fractured rock aquifer using ADFTs *in* Ground Water, 43(3), 327-335 p.

Halihan, T., Puckette, J., Sample, M., and Riley, M., 2009. Electrical resistivity imaging of the Arbuckle-Simpson Aquifer: final report *submitted to* the Oklahoma Water Resources Board, 92 p.

Hannan, J.M., 2011, Potassium-magnesium antagonism in high magnesium vineyard soils, Iowa State University, M.Sc. thesis, 40 p.

Heaton, T.H.E., 1986, Isotopic studies of nitrogen pollution in the hydrosphere and atmosphere: a review *in* Chemical Geology (Isotope Gesciences Section), 59, 87-102 p.

Heaton, T.H.E., 1987, 15N/14N ratios of nitrate and ammonium in rain at Pretoria, South Africa *in* Atmospheric Environment, 21(4), 843-852 p.

Heaton, T.H.E., Spiro, B., Madeline, S., and Robertson, C., 1997, Potential canopy influences on the isotopic composition of nitrogen and sulphur in atmospheric depostion *in* Oecologia, 109, 600-607 p.

Heinen, M., 2006, Simplified denitrification models: overview and properties *in* Geoderma, 133, 444-463 p.

Hershfield, D.M., 1963, Rainfall frequency atlas of the United States for durations from 30 minutes to 24 hours and return periods from 1 to 100 years, Weather Bureau Technical Paper No. 40: U.S. Department of Commerce, 54 p.

Hoering, T., 1957, The isotopic composition of the ammonia and the nitrate ion in rain *in* Geochemica et Cosmochimica Acta, 12, 97-102 p.

Hountin, J.A., Couillard, D., and Karam, A., 1997, Soil carbon, nitrogen and phosphorus contents in maize plots after 14 years of pig slurry applications *in* Journal of Agricultural Science, 129, 187-191 p.

Iyyemperumal, K. and Shi, W., 2008, Soil enzyme activities in two forage systems following application of different rates of swine lagoon effluent or ammonium nitrate *in* Applied Soil Ecology, 38, 128-136 p.

Johnson, C.K., Doran, J., Duke, H.R., Wienhold, B.J., and Eskridge, K., 2001, Field-scale electrical conductivity mapping for delineating soil condition *in* Soil Science America Journal, 65, 1829-1837 p.

Johnson, R.A. and Bhattacharyya, G.K., eds., 2006, Statistics: principles and methods, Hoboken NJ: John Wiley & Sons, Print.

Kaufmann, G., Romanov, D., and Nielbock, R., 2011, Cave detection using multiple geophysical methods: Unicorn cave, Harz Mountains, Germany *in* Geophysics, 76(3), B71-B77 p.

Kendall, C. and McDonnell, J.J., eds., 1998, Isotope tracers in catchment hydrology, Amsterdam: Elsevier Science B.V., Print.

King, T., Schoenau, J.J., and Malhi, S.S., 2015, Effect of application of liquid swine manure on soil organic carbon and enzyme activities in two contrasting Saskatchewan soils *in* Sustainable Agriculture Research, 4(1), 13-25 p.

Kleinman, P.J.A., Srinivasan, M.S., Dell, C.J., Schmidt, J.P., Sharpley, A.N., and Bryant, R.B., 2006, Role of rainfall intentsity and hydrology in nutrient transport via surface runoff *in* Journal of Environmental Quality, 35(4), 1248-1259 p.

Klimchouk, A., 2004, Towards defining, delimiting and classifying epikarst: its origin, processes and variants of geomorphic evolution *in* Speleogensis and Evolution of Karst Aquifers, 13 p.

Klimek, B., 2004, Effect of long-term zinc pollution on soil microbial community resistance to repeated contamination *in* Bulletin of Environmental Contamination, 88 (4), 617-622 p.

Klute, A., 1986, Methods of Soil Analysis: Part 1 – Physical and Mineralogical Methods, 2nd Ed., Madison, WI: Soil Science Society of America, Print.

Kohl, D.H., Shearer, G.B., and Commoner, B., 1971, Fertilizer nitrogen: contribution to nitrate in surface water in a corn belt watershed *in* Science, 174(4016), 1331-1334 p.

Kreitler, C.W., 1975, Determining the source of nitrate in groundwater by nitrogen isotope studies: Austin, Texas, University of Texas, Austin *in* Bureau of Economic Geology Report of Investigation #83, 57 p.

Kreitler, C.W., 1979, Nitrogen-isotope ratio studies of soils and groundwater nitrate from alluvial fan aquifers in Texas *in* Journal of Hydrology, 42, 147-170 p.

Leucci, G., 2006, Contribution of ground penetrating radar and electrical resistivity tomography to identify the cavity and fractures under the main church in Boturgno (Lecce, Italy) *in* Journal of Archaeological Science, 33, 1194-1204 p.

Lukman, S., Essa, M.H., Mu'azu, N.D., Bukhari, A., and Basheer, C., 2013, Adsorption and desorption of heavy metals onto natural clay materials: influence of initial pH *in* Journal of Environmental Science and Technology, 6(1), 1-15 p.

Luxton, T.P., Miller, B.W., and Scheckel, K.G., 2013, Speciation Studies in Soil, Sediment and Environmental Samples, Chapter 11: Zinc Speciation Studies in Soil, Sediment and Environmental Samples, Boca Raton, FL: CRC Press, Print.

Maggi, F., Gu, C., Riley, W.J., Hornberger, G.M., Venterea, R.T., Xu, T., Spycher, N., Steefel, C., Miller, N.L., and Oldenburg, C.M., 2008, A mechanistic treatment of the dominant soil nitrogen cycling processes: model development, testing, and application *in* Journal of Geophysical Research, 113, 13 p.

Mallin, M.A. and Cahoon, L.B., 2003, Industrialized animal production: a major source of nutrient and microbial pollution to aquatic ecosystems *in* Population and Environment, 24(5), 369-385 p.

Marr, J.B. and Facey, R.M., 1995, Agricultural waste *in* Water Environment Research, 67(4), 503-507 p.

Martínez-López, J., Rey, J., Dueñas, J., Hidalgo, C., and Benavente, J., 2013, Electrical tomography applied to the detection of subsurface cavities *in* Journal of Cave and Karst Studies, 75(1), 28-37 p.

McNeill, J.D., 1980, Electrical conductivity of soils and rocks: Technical Note TN-5, Geonics Limited, 22 p.

Mehlich, A., 1984, Mehlich-3 soil test extractant: a modification of Mehlich-2 extractant *in* Communications in Soil Science and Plant Analysis, 15(12), 1409-1416 p.

Mihevc, A. and Stepišnik, U., 2012, Electrical resistivity imaging of cave Divaška jama, Slovenia *in* Journal of Cave and Karst Studies, 74(3), 235-242 p.

Miller, R.B., Heeren, D.M., Fox, G.A., Halihan, T., Storm, D.E., and Mittelstet, A.R., 2014, The permeability structure of gravel-dominated alluvial floodplains *in* Journal of Hydrology, 513, 229-240 p.

Mtchell, C.C. and Everest, J.W., 1995, Soil testing & plant analysis: Southern Regional Fact Sheet, SERA-IEG-6*1, 8 p.

Moore, H., 1977, The isotopic composition of ammonia, nitrogen dioxide and nitrate in the atmosphere *in* Atmospheric Environment, 13, 1239-1243 p.

Murdock, L. and Howe, P., 2001, Zinc fertilizer rates and Mehlich III soil test levels for corn *in* Agronomy notes, 33(1), 6 p.

National Park Service, 2016, Research: Water Quality Monitoring Program: U.S. Department of the Interior, accessed May 1, 2016, at URL https://www.nps.gov/buff/learn/nature/research.htm

National Resources Conservation Service, 2008, Soil quality indicators sheet: bulk density: U.S. Department of Agriculture, 2 p.

National Weather Service Forcast Office, 2014, Little Rock, AR Climate: U.S. Department of Commerce, accessed May 1, 2016, at URL https://www.weather.gov/climate/index.php?wfo=lzk

Nielsen, D.R., Biggar, J.W., and Erh, K.T., 1973, Spatial variability of field-measured soil-water properties *in* Hilgardia, 42(7), 215-260 p.

Oh, T.-M., Cho, G.-C., and Lee, C., 2014, Effect of soil mineralogy and pore-water chemistry on the electrical resistivity of saturated soils *in* Journal of Geotechnical Geoenvironmental Engineering, Technical Note, 5 p.

Oklahoma State University Office of Intellectual Property, 2004, Improved method for Electrical Resistivity Imaging.

Paerl, H.W. and Fogel, M.L., 1994, Isotopic characterization of atmospheric nitrogen inputs as sources of enhanced primary production in coastal Atlantic Ocean waters *in* Marine Biology, 119, 635-645 p.

Pellicer, X.M. and Gibson, P., 2011, Electrical resistivity and ground penetrating radar for the characterisation of the internal architecture of Quaternary sediments in the Midlands of Ireland *in* Journal of Applied Geophysics, 75, 638-647 p.

Pettyjohn, W.A., Hagen, D.J., Ross, R., and Hounslow, A.W., 1986, Expecting the unexpected *in* paper presented at the Sixth National Symposium and Exposition on Aquifer Restoration and Ground Water Monitoring, May 19-22, 1986, Columbus, Ohio, 196-215 p.

Perelomov, L.V., Pinskly, D.L., and Violante, A., 2011, Effect of organic acids on the adsorption of copper, lead, and zinc by goetithe *in* Eurasian Soil Science, 44(1), 22-28 p.

Pérez-Novo, C., Fernández-Calviño, D., Bermúdez-Couso, A., López-Periago, J.E., Arias-Estévez, M., 2011, Phosphorus effect on Zn adsorption-desorption kinetics in acid soils *in* Chemosphere, 83, 1028-1034 p.

Perrin, J., Jeannin, P.-Y., and Zwahlen, F., 2003, Epikarst storage in a karst aquifer: a conceptual model based on isotopic data, Milandre test site, Switzerland *in* Journal of Hydrology, 279 (1-4), 106-124 p.

Plaza, C., Hernández, D., García-Gil, J.C., and Polo, A., 2004, Microbial activity in pig slurry-amended soils under semiarid conditions *in* Soil Biology & Biochemistry, 36, 1577-1585 p.

Plaza, C., Hernandez, D., and Garcia-Gil, A.P., 2004, Microbial activity in pig slurry-amended soils under semiarid conditions *in* Soil Biology and Biochemistry, 36 (10), 1577-1585 p.

Racz, G.J. and Fitzgerald, M.M., 2000, Nutrient heavy metal contents on hog manure – effect on soil quality and productivity, 21 p.

Reddy, K.R., Overcash, M.R., Khaleel, R., and Westerman, P.W., 1980, Phosphorous adsorption-desorption characteristics of two soils utilized for disposal of animal wastes *in* Journal of Environmental Quality, 9(1), 86-92 p.

Robain, H., Descloitres, M., Ritz, M., and Atangana, Q.Y., 1996, A multiscale electrical survey of a lateritic soil system in the rain forest of Cameroon *in* Journal of Applied Geophysics, 34, 237-253 p.

Samouëlian, A., Cousin, I., Tabbagh, A., Bruand, A., and Richard, G., 2005, Electrical resistivity survey in soil science: a review *in* Soil & Tillage Research, 83, 173-193 p.

Schimel, J.P. and Bennett, J., 2004, Nitrogen mineralization: challenges of a changing paradigm *in* Ecology, 85(3), 591-602 p.

Schoenau, J.J., 2006, Benefits of long-term application of manure *in* Advances in Pork Production, 17, 153 p.

Schulte, E.E., 2004, Soil and Applied Zinc, A2528, 2 p.

Schwartz, B.F. and Schreiber, M.E., 2009, Quantifying potential recharge in mantled sinkholes using ERT *in* Ground Water, 47(3), 370-381 p.

Sharp, J.M., Jr., 2007, A glossary of hydrogeological terms: Department of Geological Sciences, Austin, Texas, The University of Texas, 63 p.

Sharpley, A.N., 1985, Depth of surface soil-runoff interactions as affected by rainfall, soil slope, and management *in* Soil Science Society of America Journal, 49, 1010-1015 p.

Sharpley, A.N., 1995, Soil phosphorus dynamics: agronomic and environmental impacts *in* Ecological Engineering, 5, 261-279 p.

Sharpley, A.N., Daniels, M., VanDevender, K., and Slaton, N., 2010, Soil phosphorus: management and recommendations, FSA1029, 6 p.

Shearer, G.B., Kohl, D.H., and Commoner, B., 1974, The precision of determinations of the natural abundance of nitrogen-15 in soils, fertilizers, and shelf chemicals *in* Soil Science, 118(5), 308-316 p.

Shearer, G.B., Kohl, D.H., and Chien, S.-H., 1978, The nitrogen-15 abundance in a wide variety of soils *in* Soil Science Society of America Journal, 42(6), 899-902 p.

Smart, P.L., and Friederich, H., 1986, Water movement and storage in the unsaturated zone of a maturely karstified carbonate aquifer, Mendip Hills England *in* conference proceedings on: Environmental problems of Karst Terrains and their solutions, National Water Well Association, Ohio, 59-87 p.

Smith, D.R., Owens, P.R., Leytem, A.B., and Warnemuende, E.A., 2007, Nutrient losses from manure and fertilizer applications as impacted by time to first runoff event, *in* Environmental Pollution, 147, 131-137 p.

Steefel, C.I., DePaolo, D.J., and Lichtner, P.C., 2005, Reactive transport modeling: an essential tool and a new research approach for the Earth sciences *in* Earth and Planetary Science Letters, 240, 539-558 p.

Stepisnik, U. and Mihevc, A., 2008, Investigation of structure of various surface karst formations in limestone and dolomite bedrock with application of the electrical resistivity imaging *in* Acta Carsologica, 37(1), 133-140 p.

Sudha, K., Israil, M., Mittal, S., and Rai, J., 2009, Soil characterization using electrical resistivity tomography and geotechnical investigations *in* Journal of Applied Geophysics, 67, 74-79 p.

Suhadolc, M., Schroll, R., Gattinger, A., Schloter, M., Munch, J.C., and Lestan, D., 2004, Effects of modified Pb-, Zn-, and Cd-, availability on the microbial communities and on the degradation of isoproturon in a heavy metal contaminated soil *in* Soil Biology and Biochemistry, 36, 1943-1954 p.

Tsoflias, G.P., and Becker, M.W., 2008, Ground-penetrating-radar response to fracture-fluid salinity: why lower frequencies are favorable for resolving salinity changes *in* Geophysics, 73(5), J25-J30 p.

Turner, J.C., Hattey, J.A., Warren, J.G., and Penn, C.J., 2010, Electrical conductivity and sodium adsorption ratio changes following annual applications of animal manure amendments *in* Communications in Soil Science and Plant Analysis, 41, 1043-1060 p.

U.S. Geological Survey, 2015, Water Science Glossary of Terms (The USGS Water Science School): U.S. Department of the Interior, accessed July 1, 2015, at URL http://water.usgs.gov/edu/dictionary.html

U.S. Geological Survey, 2014, Geologic Glossary (USGS Geology in the Parks): U.S. Department of the Interior, accessed July 1, 2015, at URL http://geomaps.wr.usgs.gov/parks/misc/glossarya.html

U.S. Salinity Laboratory Staff, 1954, Diagnosis and Improvement of Saline and Alkali Soils *in* USDA Agriculture Handbook No. 60., 84-89 p.

Vadas, P.A., Gburek, W.J., Sharpley, A.N., Kleinman, P.J.A., Moore, P.A., Jr., Cabrera, M.L., and Harmel, R.D., 2007, A model for phosphorus transformation and runoff loss for surface-applied manures *in* Journal of Environmental Quality, 36(1), 324-332 p.

Van Nostrand, R.G. and Cook, K.L., 1966, Interpretation of resistivity data: U.S. Geological Survey Professional Paper 499, 307 p.

van Schoor, M., 2002, Detection of sinkholes using 2D electrical resistivity imaging *in* Journal of Applied Geophysics, 50, 393-399 p.

Vanderhoff, S.M., 2011, Multiple storm event impacts on epikarst storage and transport of organic soil amendments in south-central Kentucky, Western Kentucky University, M.Sc. Thesis, 67 p.

Vitousek, P.M., Aber, J.D., Howarth, R.W., Likens, G.E., Matson, P.A., Schindler, D.W., Schlesinger, W.H., Tilman, D.G., 1997, Human alteration of the global nitrogen cycle: sources and consequences *in* Ecological Applications, 7(3), 737-750 p.

Wallenius, K., Rita, H., Mikkonen, A., Lappi, K., Lindstrom, K., Hartikainen, H., Raateland, A., and Niemi, R.M., 2011, Effects of land use on the level, variation and spatial structure of soil enzyme activities and bacterial communities *in* Soil Biology & Biochemistry, 43, 1464-1473 p.

Whetstone Associates, Inc., 2011, EnergySolutions class a west disposal cell infiltration and transport modeling report *submitted to* EnergySolutions, LLC, Document Number 4101M.110419, 60 p.

Williams, P.W., 1985, Subcutaneous hydrology and the development of doline and cockpit karst. Zeitschrift fur Geomorphologie, 29, 463-482 p.

Williams, P.W., 2008, The role of the epikarst in karst and cave hydrogeology *in* International Journal of Speleology, 37(1), 10 p.

Wolterink, T.J., Williamson, H.J., Jones, D.C., Grimshaw, T.W., and Holland, W.F., 1979, Identifying sources of subsurface nitrate pollution with stable nitrogen isotopes: U.S. Environmental Protection Agency, EPA-600/4-79-050, 150 p.

Xu, T., Sonnenthal, E., Spycher, N., and Pruess, K., 2003, TOUGHREACT: a new code of the TOUGH family for non-isothermal multiphase reactive geochemical transport in variably saturated geologic media, Lawrence Berkeley National Laboratory, accessed May 1, 2016, at URL http://escholarship.org/uc/item/4qp0k69n

Xu, T., Spycher, N., Sonnenthal, E., Zhang, G., Zheng, L., and Pruess, K., 2010, TOUGHREACT Version 2.0: a simulator for subsurface reactive transport under non-isothermal multiphase flow conditions, Lawrence Berkeley National Laboratory, accessed May 1, 2016, at URL http://escholarship.org/uc/item/9tw7m3rj

Yadav, S.N., 1997, Formulation and estimation of nitrate-nitrogen leaching from corn cultivation *in* Journal of Environmental Quality, 26(3), 808-814 p.

Youssef, A.M., El-Kaliouby, H., and Zabramawi, Y.A., 2012, Sinkhole detection using electrical resistivity tomography in Saudi Arabia *in* Journal of Geophysical Engineering, 9, 655-663 p.

Zhang, H., 1998, Animal manure can raise soil pH, PT 98-7, 2 p.

Zhang, H., 2002, Understanding your soil test report, PT 2002-10, 2 p.

Zhang, H., n.d., Fertilizer nutrients in animal manure, PSS-2228, 2 p.

Zhang, H. and Henderson, K., 2015, Procedures used by OSU Soil, Water, and Forage Analytical Laboratory, PSS-2901, 4 p.

Zhang, H. and Stiegler, J., 1998, Animal manure and soil quality, PT 98-8, 3 p.

Zhou, W., Beck, B.F., and Stephenson, J.B., 2000, Reliability of dipole-dipole electrical resistivity tomography for defining depth to bedrock in covered karst terranes *in* Environmental Geology, 39(7), 760-766 p.

Zhu, J., Currens, J.C., and Dinger, J.S., 2011, Challenges of using electrical resistivity method to locate karst conduits – a field case in the Inner Bluegrass Region, Kentucky *in* Journal of Applied Geophysics, 75, 523-530 p.

9.0 ELECTRONIC APPENDICIES

Appendix 1: Geodetic Data (Microsoft Excel format)

Appendix 2: ERI raw modeled data (Microsoft Excel format)

Appendix 3: ERI images (PDF format)

Appendix 4: 3D Site Models (RockWare RockWorks format)

Appendix 5: Site Photos (PDF format)

Appendix 6: Soil Analysis (Microsoft Excel format)

VITA

Jon Jay Fields Jr.

Candidate for the Degree of

Master of Science

Thesis: HYDROGEOPHYSICAL CHARACTERIZATION OF SWINE EFFLUENT AMENDED SOILS IN MANTLED KARST

Major Field: Geology

Biographical:

Born in Raleigh, North Carolina on September 14th, 1990 to Jon Jay Fields Sr. and Kristi Michele Fields.

Education:

Completed the requirements for the Master of Science in Geology at Oklahoma State University, Stillwater, Oklahoma in May, 2016.

Completed the requirements for the Bachelor of Science in Geology at Oklahoma State University, Stillwater, Oklahoma in 2014.

Completed the requirements for a high school diploma at Lawton Senior High School, Lawton, Oklahoma in 2009.

Experience:

Graduate Teaching Assistant, Boone Pickens School of Geology, Oklahoma State University, August 2015 to December 2016.

Graduate Research Assistant, Boone Pickens School of Geology, Oklahoma State University, January 2015 to September 2015.

Undergraduate Teaching Assistant, Boone Pickens School of Geology, Oklahoma State University, January 2014 to May 2014.